

CHAPTER 9**Wave-Mean Flow Interactions**

Copyright 2003 David A. Randall

9.1 Interactions and non-interactions of gravity waves with the mean flow.

We have seen how eddies can affect the mean flow, through eddy flux divergences and energy conversions. Despite the presence of such terms in the equations, however, it turns out that under surprisingly general conditions the eddies are actually powerless to affect the mean flow. There are several related theorems that demonstrate this “non-interaction” of the eddies with the mean flow. They are called, reasonably enough, “non-interaction theorems.” The earliest such ideas were published by Eliassen and Palm (1961), and the following discussion is based on their paper. This same material is also discussed at length in Lindzen’s (1990) book.

Consider the equation of zonal motion in the simplified form

$$\frac{\partial u}{\partial t} + u \frac{\partial u}{\partial x} + w \frac{\partial u}{\partial z} = -\frac{1}{\rho} \frac{\partial p}{\partial x} . \quad (9.1)$$

We have omitted rotation, sphericity, friction, and y-variations for simplicity. Eq. (9.1) can apply, for example, to small-scale gravity waves forced by flow over topography. Let

$$\left. \begin{aligned} u &= U + u', & U &= U(z) \\ w &= w' \\ \bar{p} &= \bar{p} + p', & \bar{p} &= \bar{p}(z) \\ \bar{\rho} &= \bar{\rho} + \rho', & \bar{\rho} &= \bar{\rho}(z) \end{aligned} \right\} . \quad (9.2)$$

We interpret the primed quantities as small-amplitude wave-like perturbations with zero means. Recall that

$$\rho \frac{\partial U}{\partial t} \sim -\frac{\partial}{\partial z} \overline{\rho w' u'} . \quad (9.3)$$

We are going to be interested in what determines the wave momentum flux divergence, $\frac{\partial}{\partial z} \overline{\rho w' u'}$.

Substitute (9.2) into (9.1) and linearize, to obtain

$$\bar{\rho} \frac{\partial u'}{\partial t} + \bar{\rho} U \frac{\partial u'}{\partial x} + \bar{\rho} w' \frac{\partial U}{\partial z} + \frac{\partial p'}{\partial x} = 0. \quad (9.4)$$

Assume that the perturbations are *steady*, so that

$$\frac{\partial u'}{\partial t} = 0. \quad (9.5)$$

This implies both that the waves are *neutral*, i.e. neither amplifying or decaying, and also that they are *stationary*, i.e. their phase speed is zero. The latter assumption is reasonable, e.g., for mountain waves. Then

$$\bar{\rho} U \frac{\partial u'}{\partial x} + \bar{\rho} w' \frac{\partial U}{\partial z} + \frac{\partial p'}{\partial x} = 0. \quad (9.6)$$

Multiply (9.6) by $(\rho U u' + p')$, to obtain

$$\bar{\rho} U^2 \frac{\partial}{\partial x} \left(\frac{u'^2}{2} \right) + \bar{\rho}^2 w' u' \frac{\partial}{\partial z} \left(\frac{U^2}{2} \right) + \bar{\rho} U \frac{\partial}{\partial x} (p' u') + \bar{\rho} w' p' \frac{\partial U}{\partial z} + \frac{\partial}{\partial x} \left(\frac{1}{2} p'^2 \right) = 0. \quad (9.7)$$

The terms involving $\frac{\partial}{\partial x}$ vanish when we integrate over the whole domain, leaving

$$\frac{\partial}{\partial z} \left(\frac{U^2}{2} \right) \int_{-\infty}^{\infty} \bar{\rho} w' u' dx + \frac{\partial U}{\partial z} \int_{-\infty}^{\infty} w' p' dx = 0, \quad (9.8)$$

which can be simplified to

$$U \int_{-\infty}^{\infty} \bar{\rho} w' u' dx + \int_{-\infty}^{\infty} w' p' dx = 0, \quad (9.9)$$

provided that $\frac{\partial U}{\partial z} \neq 0$.

Eq. (9.9) is an important result. It means that the wave momentum flux, $\int_{-\infty}^{\infty} \bar{\rho} w' u' dx$,

and the wave energy flux, $\int_{-\infty}^{\infty} w' p' dx$, are closely related. At a “critical” level where $U = 0$,

the wave energy flux must vanish; the only other possibility is that our assumptions, e.g. a steady state with no friction, do not apply at the critical level. For a wave forced by flow over a mountain, the energy flux is, of course, upward, but (9.9) shows that it goes to zero at a critical level. This means that the wave does not exist above the critical level. The upward propagation of the wave is blocked at the critical level.

Let q be the total energy associated with the wave (the sum of the kinetic, internal, and potential energies). We can show that q satisfies

$$\frac{\partial}{\partial x}(qU + p'u') + \frac{\partial}{\partial z}(p'w') = -\bar{\rho}u'w'\frac{\partial U}{\partial z}. \quad (9.10)$$

The right-hand side of (9.10) is a “gradient production” term that represents conversion of the kinetic energy of the mean state into the total eddy energy, q . Eq. (9.10) simply says that the production term on the right-hand side is balanced by the transport terms on the left-hand side. Integration over the domain gives

$$\frac{\partial}{\partial z} \int_{-\infty}^{\infty} p'w' dx = -\frac{\partial U}{\partial z} \int_{-\infty}^{\infty} \bar{\rho}u'w' dx. \quad (9.11)$$

This means that the wave energy flux divergence balances conversion to or from the kinetic energy of the mean flow.

By combining (9.9) and (9.11) we can show that

$$U \frac{\partial}{\partial z} \left(\int_{-\infty}^{\infty} \bar{\rho}u'w' dx \right) = 0. \quad (9.12)$$

This means that, when $U \neq 0$, the wave momentum flux $\int_{-\infty}^{\infty} \bar{\rho}u'w' dx$ is independent of height. This is a very important result, because, as shown by (9.3), it means that the wave momentum flux has no effect on $U(z)$, *except at the critical level where $U = 0$* . The wave momentum flux is absorbed at the critical level. From (9.3), it follows that U will tend to change with time at the critical level, so U will become different from zero. This means that *the critical level will move*.

If we allowed the phase speed c to be non-zero, we would find $U - c$ everywhere in place of U . The momentum would be absorbed at the critical level where $U = c$.

Since (9.12) tells us that $\int_{-\infty}^{\infty} \bar{\rho}u'w' dx$ is independent of height (where $U \neq 0$), we see

from (9.9) that the wave energy flux is just proportional to U . Alternatively, we can combine (9.9) and (9.12) to write

$$\frac{1}{U} \int_{-\infty}^{\infty} w' p' dx = \text{constant}. \quad (9.13)$$

The conserved quantity $\frac{1}{U} \int_{-\infty}^{\infty} w' p' dx$ is called the “wave action.” Note that (9.9) can be written as “wave action plus wave momentum flux = zero.”

Since the mid-1980s, there has been a lot of interest in the effects of gravity wave momentum fluxes on the general circulation; because the waves act to decelerate the mean flow, these interactions are referred to as “gravity wave drag” (McFarlane, 1987). Most of the discussion so far has been on gravity waves forced by flow over topography, although recently gravity waves forced by convective storms are receiving a lot of attention (e.g. Fovell et al., 1992).

Fig. 9.1 shows the deceleration of the zonally averaged zonal wind induced by

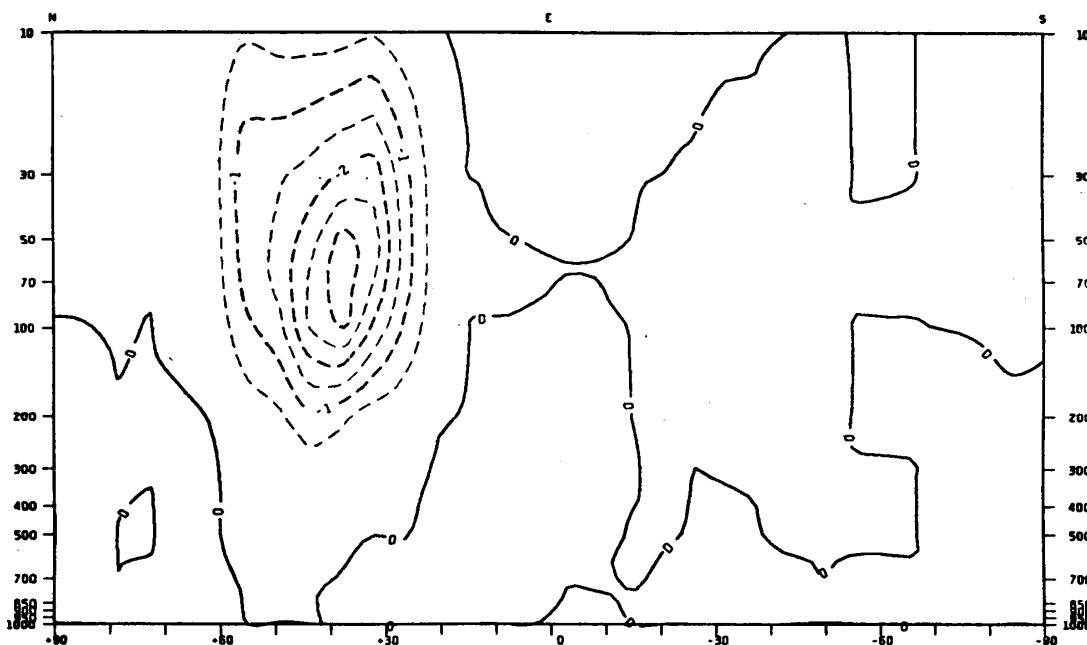


Figure 9.1: The deceleration of the zonally averaged zonal flow, induced by orographically forced gravity waves, as simulated with a general circulation model. The units are $\text{m s}^{-1} \text{ day}^{-1}$. From McFarlane (1987).

gravity-wave drag in a general circulation model, as reported by McFarlane (1987). Here the gravity wave drag has been parameterized using methods that we will not discuss, which are based on the assumption that the waves are produced by flow over mountains. The plot shows the “tendency” of the zonally averaged zonal wind due to this orographic gravity-wave drag, for northern-winter conditions. The actual response of the zonally averaged zonal wind is shown in Fig. 9.2. The changes are very large. In order for thermal wind balance to be

maintained, there must be corresponding changes in the zonally averaged temperature; these are shown in Fig. 9.3. The polar troposphere has warmed dramatically, to be consistent with the weaker westerly jet. The changes shown in Fig. 9.2 and Fig. 9.3 make the model results more realistic than before, suggesting that gravity-wave drag is an important process in nature.

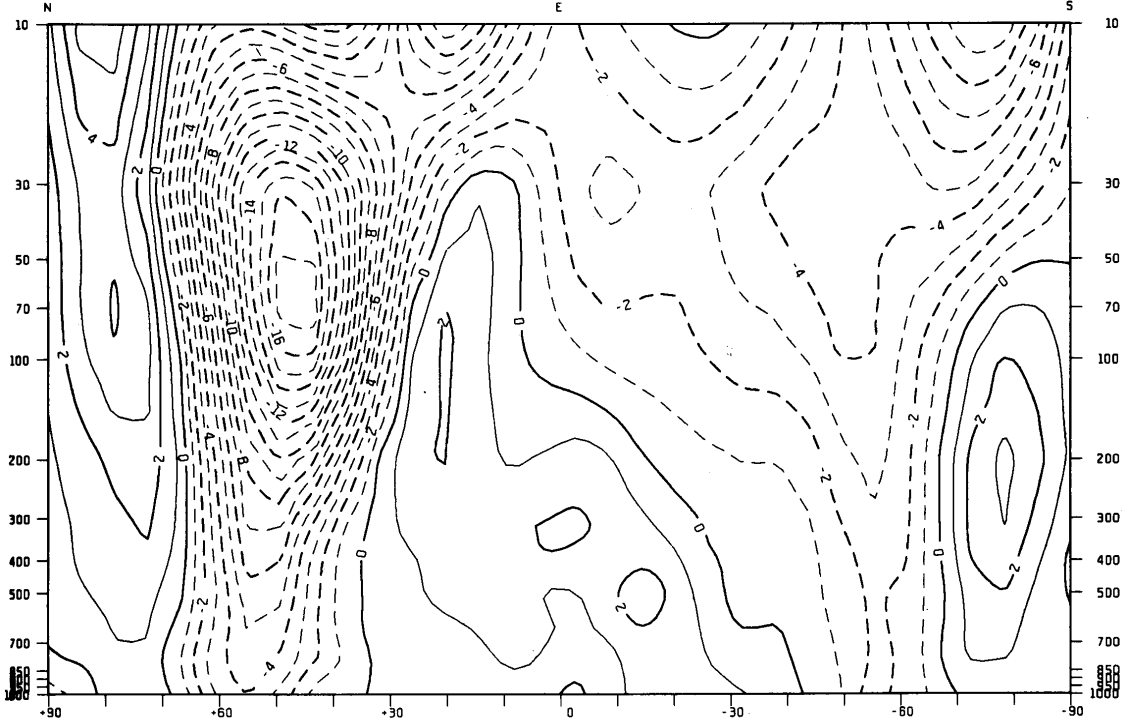


Figure 9.2: The actual change in the zonally averaged zonal wind caused by the introduction of gravity wave drag in a general circulation model, as inferred by comparison with a control run. The units are m s^{-1} . From McFarlane (1987).

9.2 Vertical propagation of planetary waves

The following discussion is based on the famous paper by Charney and Drazin (1961), which deals with the vertical propagation of planetary waves.

Let $T_S(p)$ be a standard temperature profile, and define α_S , θ_S , and ρ_S accordingly. The quasigeostrophic form of the potential vorticity equation is

$$\left(\frac{\partial}{\partial t} + \mathbf{V}_g \cdot \nabla_p \right) q = 0, \quad (9.14)$$

where

$$q = f + \xi_g + \frac{\partial}{\partial p} \left(\frac{f_0}{S_p} \frac{\partial \Phi}{\partial p} \right) \quad (9.15)$$

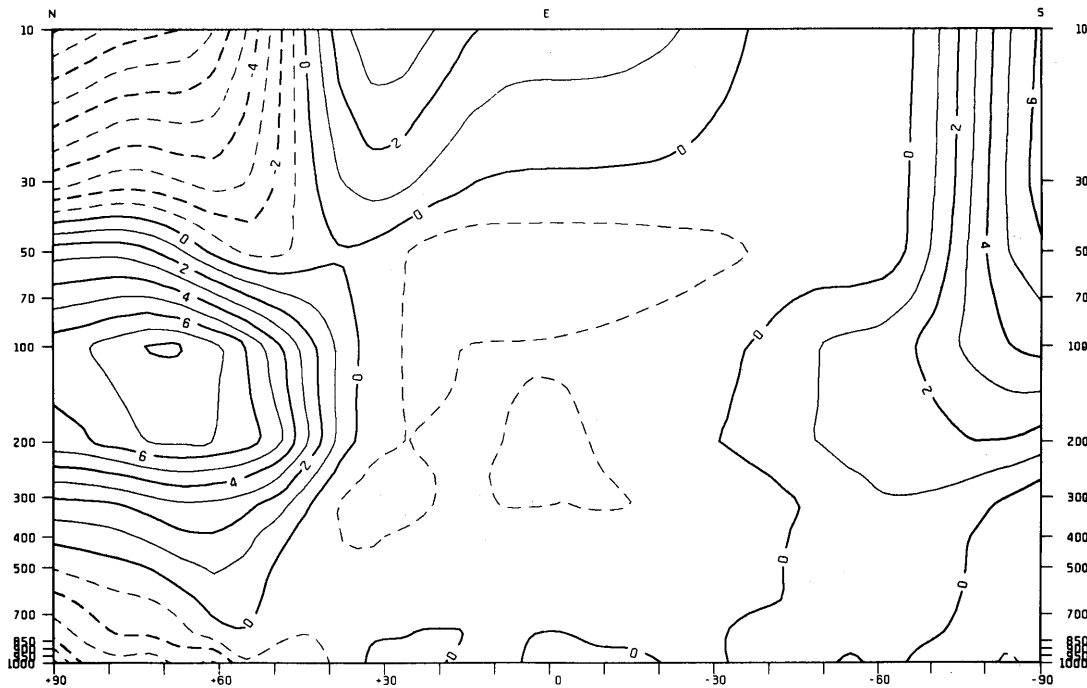


Figure 9.3: The actual change in the zonally averaged temperature caused by the introduction of gravity wave drag in a general circulation model, as inferred by comparison with a control run. The units are K^{-1} . The From McFarlane (1987).

is the quasigeostrophic pseudo-potential vorticity, $S_p \equiv -\frac{\alpha_S \partial \theta_S}{\theta_S \partial p}$ is the static stability, and in

the last term of (9.15) f has been replaced by f_0 . [See Chapter 8 of Holton (1992).] We are working on a β -plane, such that $f = f_0 + \beta y$. Note that q is essentially determined by the absolute vorticity and the change of temperature with height, and that (9.14) does not contain a vertical advection term.

From (9.14) we can derive

$$\frac{\partial}{\partial t}[q] = -\frac{\partial}{\partial y}[v_g^* q^*]. \quad (9.16)$$

EXERCISE: Show that

$$\begin{aligned}
[v_g^* q^*] &= [v_g^* \xi_g^*] - \frac{\partial}{\partial p} \left(\frac{Rf_0}{pS_p} [v_g^* T^*] \right) \\
&= -\frac{\partial}{\partial y} [u_g^* v_g^*] - \frac{\partial}{\partial p} \left(\frac{Rf_0}{pS_p} [v_g^* T^*] \right).
\end{aligned} \tag{9.17}$$

Eq. (9.17) is a very important relationship. It shows that the meridional eddy flux of potential vorticity is related to the convergence of the meridional eddy flux of zonal momentum, and to the rate of change with height of the meridional eddy sensible heat flux. When we form the convergence of the eddy potential vorticity flux, i.e. $-\frac{\partial}{\partial y} [v_* q_*]$, (9.17) will give us

$\frac{\partial}{\partial y} \left\{ -\frac{\partial}{\partial y} [u_* v_*] \right\}$. This affects the meridional shear of $[u]$. We will also get a term proportional to $\frac{\partial}{\partial p} \left\{ -\frac{\partial}{\partial y} [v_* T_*] \right\}$. This affects the static stability.

We adopt the “log pressure” coordinate

$$z(p) \equiv -\left(\frac{RT_0}{g} \right) \ln \left(\frac{p}{p_0} \right), \tag{9.18}$$

where T_0 is a constant reference temperature. With the use of (9.18), (9.15) can be rewritten as

$$q = f + \nabla^2 \psi + \frac{1}{\rho_s} \frac{\partial}{\partial z} \left(\rho_s \frac{f_0^2}{N^2} \frac{\partial \psi}{\partial z} \right), \tag{9.19}$$

where

$$\psi \equiv \frac{\phi}{f_0} \tag{9.20}$$

is called the “geostrophic stream function,” and

$$N^2 \equiv \frac{g}{\theta_s} \frac{\partial \theta_s}{\partial z}, \tag{9.21}$$

where N is the Brunt-Vaisala frequency. Note that

$$v_g = \frac{\partial \Psi}{\partial x} \text{ and } u_g = -\frac{\partial \Psi}{\partial y}. \quad (9.22)$$

Linearizing (9.14) about the zonal-mean state gives

$$\left(\frac{\partial}{\partial t} + [u] \frac{\partial}{\partial x} \right) q_* + v_* \frac{\partial}{\partial y} [q] = 0. \quad (9.23)$$

We look for solutions of the form

$$\Psi^* = \text{Re} \{ \hat{\Psi}(y, z) e^{ik(x-ct)} \}, \quad (9.24)$$

$$q^* = \text{Re} \{ \hat{q}(y, z) e^{ik(x-ct)} \}. \quad (9.25)$$

Substitution of (9.19), (9.24), and (9.25) into (9.23) gives

$$([u] - c) \hat{q} + \hat{\Psi} \frac{\partial}{\partial y} [q] = 0, \quad (9.26)$$

where

$$\hat{q} = -k^2 \hat{\Psi} + \frac{\partial^2 \hat{\Psi}}{\partial y^2} + \frac{1}{\rho_S} \frac{\partial}{\partial z} \left(\rho_S \frac{f_0^2}{N^2} \frac{\partial \hat{\Psi}}{\partial z} \right). \quad (9.27)$$

Using (9.27), we can rewrite (9.26) as

$$\frac{\partial^2}{\partial y^2} \hat{\Psi} + \frac{1}{\rho_S} \frac{\partial}{\partial z} \left(\rho_S \frac{f_0^2}{N^2} \frac{\partial \hat{\Psi}}{\partial z} \right) = - \left(\frac{1}{[u] - c} \frac{\partial [q]}{\partial y} - k^2 \right) \hat{\Psi}. \quad (9.28)$$

This is a fairly general form of the quasi-geostrophic wave equation that we want to analyze, but we will simplify it considerably before doing so.

As wave energy propagates up to higher levels, it encounters decreasing values of ρ_S . The energy-density (energy per unit volume) scales like $\rho_S (k\Psi)^2$, so if the energy density is constant with height, $\hat{\Psi}$ must increase like $\frac{1}{\sqrt{\rho_S}}$. Because of this effect, the equations become simpler if we introduce a scaled value of Ψ :

$$\Psi \equiv \frac{\sqrt{\rho_S}}{N} \hat{\Psi}. \quad (9.29)$$

Note that here ψ (no hat) is the scaled value; the meaning of ψ now departs from that used in (9.20). We also note that

$$\begin{aligned}
 \frac{1}{\rho_s} \frac{\partial}{\partial z} \left(\rho_s \frac{f_0^2}{N^2} \frac{\partial \hat{\psi}}{\partial z} \right) &= \frac{f_0^2}{\rho_s} \frac{\partial}{\partial z} \left\{ \frac{\sqrt{\rho_s}}{N} \frac{\partial}{\partial z} \left(\frac{\sqrt{\rho_s}}{N} \hat{\psi} \right) - \frac{\sqrt{\rho_s}}{N} \hat{\psi} \frac{\partial}{\partial z} \left(\frac{\sqrt{\rho_s}}{N} \right) \right\} \\
 &= \frac{f_0^2}{\rho_s} \left\{ \frac{\partial}{\partial z} \left(\frac{\sqrt{\rho_s}}{N} \right) \frac{\partial}{\partial z} \left(\frac{\sqrt{\rho_s}}{N} \hat{\psi} \right) + \frac{\sqrt{\rho_s}}{N} \frac{\partial^2}{\partial z^2} \left(\frac{\sqrt{\rho_s}}{N} \hat{\psi} \right) \right. \\
 &\quad \left. - \frac{\partial}{\partial z} \left(\frac{\sqrt{\rho_s}}{N} \hat{\psi} \right) \frac{\partial}{\partial z} \left(\frac{\sqrt{\rho_s}}{N} \right) - \left(\frac{\sqrt{\rho_s}}{N} \hat{\psi} \right) \frac{\partial^2}{\partial z^2} \left(\frac{\sqrt{\rho_s}}{N} \right) \right\} \\
 &= \frac{f_0^2}{\rho_s} \left[\frac{\sqrt{\rho_s}}{N} \frac{\partial^2}{\partial z^2} \psi - \psi \frac{\partial^2}{\partial z^2} \left(\frac{\sqrt{\rho_s}}{N} \right) \right].
 \end{aligned} \tag{9.30}$$

Using (9.29) and (9.30), we can rewrite (9.28) as

$$\frac{\partial^2 \psi}{\partial y^2} + \frac{f_0^2}{N^2} \frac{\partial^2 \psi}{\partial z^2} = -\frac{f_0^2}{N^2} \frac{1}{4H_0^2} n^2 \psi, \tag{9.31}$$

where

$$n^2 \equiv \frac{4N^2 H_0^2}{f_0^2} \left\{ \frac{1}{[u] - c} \frac{\partial [q]}{\partial y} - k^2 - \frac{f_0^2}{\sqrt{\rho_s} N} \frac{\partial^2}{\partial z^2} \left(\frac{\sqrt{\rho_s}}{N} \right) \right\} \tag{9.32}$$

is called the “index of refraction.” Here $H_0 \equiv \frac{RT_0}{g}$, where T_0 is a reference temperature.

Comparing (9.31) - (9.32) with (9.28), it seems that the left-hand side has been simplified but the right-hand side has become more complicated., Eq. (9.32) is a form of the quasigeostrophic wave equation. When $n^2 > 0$, ψ is oscillatory (propagating), and when $n^2 < 0$, ψ is “evanescent” (exponentially decaying away from the source of excitation).

The index of refraction as given by (9.32) is pretty complicated. Consider a simplified special case: an isothermal atmosphere with $T_S(p) \equiv T_0 = \text{constant}$. This is not unrealistic

for the lower stratosphere. For this case, we can show that $N \equiv \text{constant}$ and $\rho_S \sim e^{-\frac{z}{H_0}}$, so that (9.32) can be simplified to

$$n^2 \equiv \frac{4N^2 H_0^2}{f_0^2} \left(\frac{1}{[u] - c} \frac{\partial[q]}{\partial y} - k^2 \right) - 1 . \quad (9.33)$$

Now we concentrate on stationary waves, for which the phase speed, c , is zero. This type of wave can be forced by orography, for example, as discussed in Chapter 7. Then (9.31) and (9.33) become

$$\frac{\partial^2 \Psi}{\partial y^2} + \frac{f_0^2}{N^2} \frac{\partial^2 \Psi}{\partial z^2} = -\frac{n^2}{4H_0^2} \Psi , \quad (9.34)$$

$$n^2 = \frac{4N^2 H_0^2}{f_0^2} \left(\frac{1}{[u]} \frac{\partial[q]}{\partial y} - k^2 \right) - 1 . \quad (9.35)$$

To simplify n^2 even further, note from (9.19) that

$$\frac{\partial}{\partial y}[q] = \beta - \frac{\partial^2 [u]}{\partial y^2} - \frac{1}{\rho_S} \frac{\partial}{\partial z} \left(\rho_S \frac{f_0^2}{N^2} \frac{\partial [u]}{\partial z} \right) , \quad (9.36)$$

where $\beta \equiv \frac{df}{dy}$. When the variations of $[u]$ are not too strong,

$$\partial[q]/\partial y \equiv \beta \geq 0 . \quad (9.37)$$

Then

$$n^2 \equiv \frac{4N^2 H_0^2}{f_0^2} \left(\frac{\beta}{[u]} - k^2 \right) - 1 . \quad (9.38)$$

From (9.38), we see the following:

- To have vertical propagation ($n^2 > 0$), we need $\beta/[u] > 0$. Because $\beta > 0$, $[u]$ must be positive (westerly). *Stationary Rossby waves cannot propagate through easterlies.* Recall that the summer hemisphere stratosphere is dominated by easterlies, while the winter hemisphere stratosphere is dominated by westerlies. Note, however, that *large* positive $[u]$ also makes

$n^2 < 0$. Waves cannot propagate through very strong westerlies. Fig. 9.4, from Charney and Drazin (1961), shows the vertical distribution of n^2 for summer and winter, averaged over the Northern Hemisphere middle latitudes, for three different wavelengths.

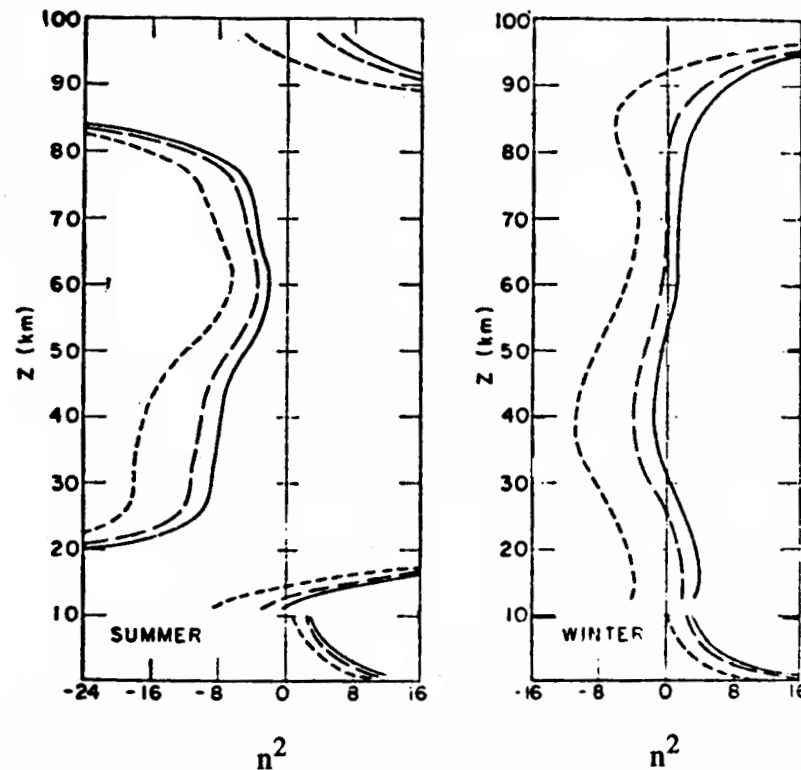


Figure 9.4: The square of the index of refraction for summer and winter, averaged between 30° and 60°N , for waves of different wavelengths, L . The short-dashed lines correspond to $L = 6,000$ km, the long-dashed lines correspond to $L = 10,000$ km, and the solid lines correspond to $L = 14,000$ km. From Charney and Drazin (1961).

- Even when $\beta/[u] > 0$, for a given $[u]$ waves with sufficiently large k (short wavelength) cannot propagate. Short waves are, therefore, “trapped” near their excitation levels. Since $[u]$ has a *maximum* near the tropopause in middle latitudes, many short waves are trapped in the troposphere, even in winter. Only longer waves can propagate to great heights. This suggests that long waves will dominate the stratosphere and mesosphere even more than they do in the troposphere.
- A level where $[u] = 0$ is called a “critical level” for stationary waves. Suppose

that $[u] > 0$ below a critical level, and $[u] < 0$ above. Then, for waves excited at the lower boundary (e.g., by topography), upward propagation is *completely blocked* at the critical level.

Fig. 9.5 provides evidence that the theory is correct. It shows the geopotential height fields at 500 mb, 100 mb, and 10 mb, for Northern Hemisphere summer and winter. In winter, planetary waves clearly propagate upward to the 10 mb level, while in summer they do not. Note that the apparent horizontal scale of the dominant eddies increases upward, in winter. This is consistent with the theory, which predicts that the shorter modes are trapped at lower levels while longer modes can continue to propagate upward to great heights.

Waves can also be trapped at *critical latitudes* where $[u] = 0$. We could therefore define *critical surfaces* in the y - z plane.

If we allowed $c \neq 0$, we would find that the critical surfaces are those for which $[u] - c = 0$.

Matsuno (1970) used $[u]$ for the Northern Hemisphere winter to compute $\frac{\partial[q]}{\partial\phi}$, the index of refraction, and the energy flow in the latitude-height plane for zonal wave number 1. His results are shown in Fig. 9.6.

Fig. 9.7 shows that planetary wave energy does in fact propagate from the troposphere into the stratosphere during northern winter.

Fig. 9.8 shows that the eddy kinetic energy in the stratosphere is supplied by the troposphere. KZ is converted into AZ , i.e. the meridional temperature gradient is increased by an indirect circulation. The general circulation of the lower stratosphere thus acts like a refrigerator.

9.3 Vertical and meridional fluxes due to planetary waves

Now we investigate under what conditions planetary waves can transport energy and momentum. The quasigeostrophic form of the thermodynamic energy equation is (e.g. Holton, 1992)

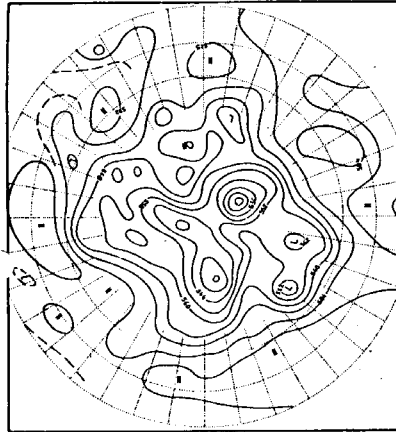
$$\left(\frac{\partial}{\partial t} + \mathbf{V} \cdot \nabla\right) \frac{\partial\phi}{\partial p} + S_p \omega = 0. \quad (9.39)$$

(Here \mathbf{V} is the geostrophic wind and ∇ is ∇_p .) Eq. (9.39) can be written as

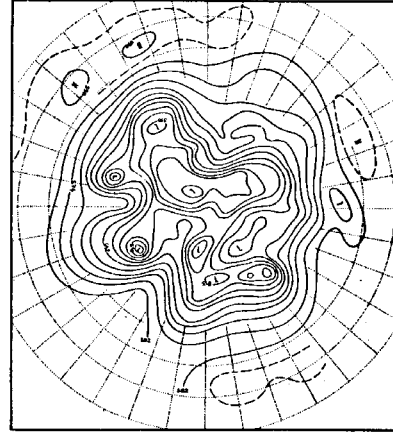
$$\left(\frac{\partial}{\partial t} + \mathbf{V} \cdot \nabla\right) \psi_z + \frac{N^2}{f_0} w = 0, \quad (9.40)$$

where w is defined by $-\omega/(\rho_s g)$. Here $\psi_z \equiv \partial\psi/\partial z$, and z is the “log- p ” coordinate defined by (9.18). Linearizing (9.40) gives

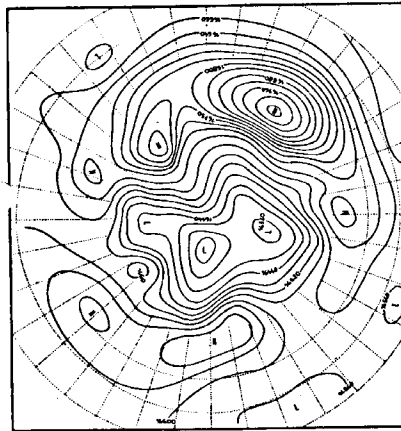
July 15, 1958, 500 mb



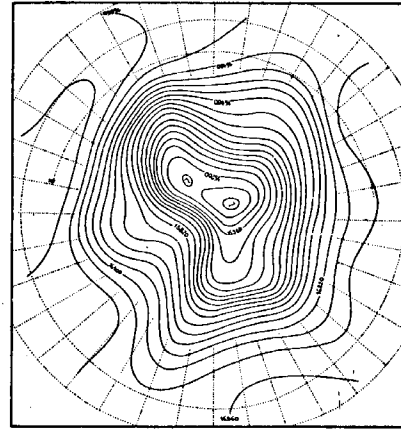
January 15, 1959, 500 mb



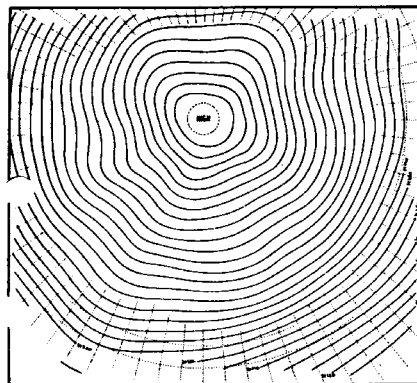
July 15, 1958, 100 mb



January 15, 1959, 100 mb



July 15, 1958, 10 mb



January 15, 1959, 10 mb

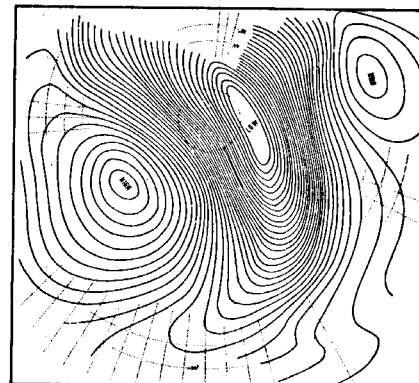


Figure 9.5: These Northern Hemisphere data were collected during the International Geophysical Year. Geopotential heights for July 15 1958 are shown on the left, and those for January 15 1959 are shown on the right. The levels plotted are 500 mb, 100 mb, and 10 mb. From Charney (1973).

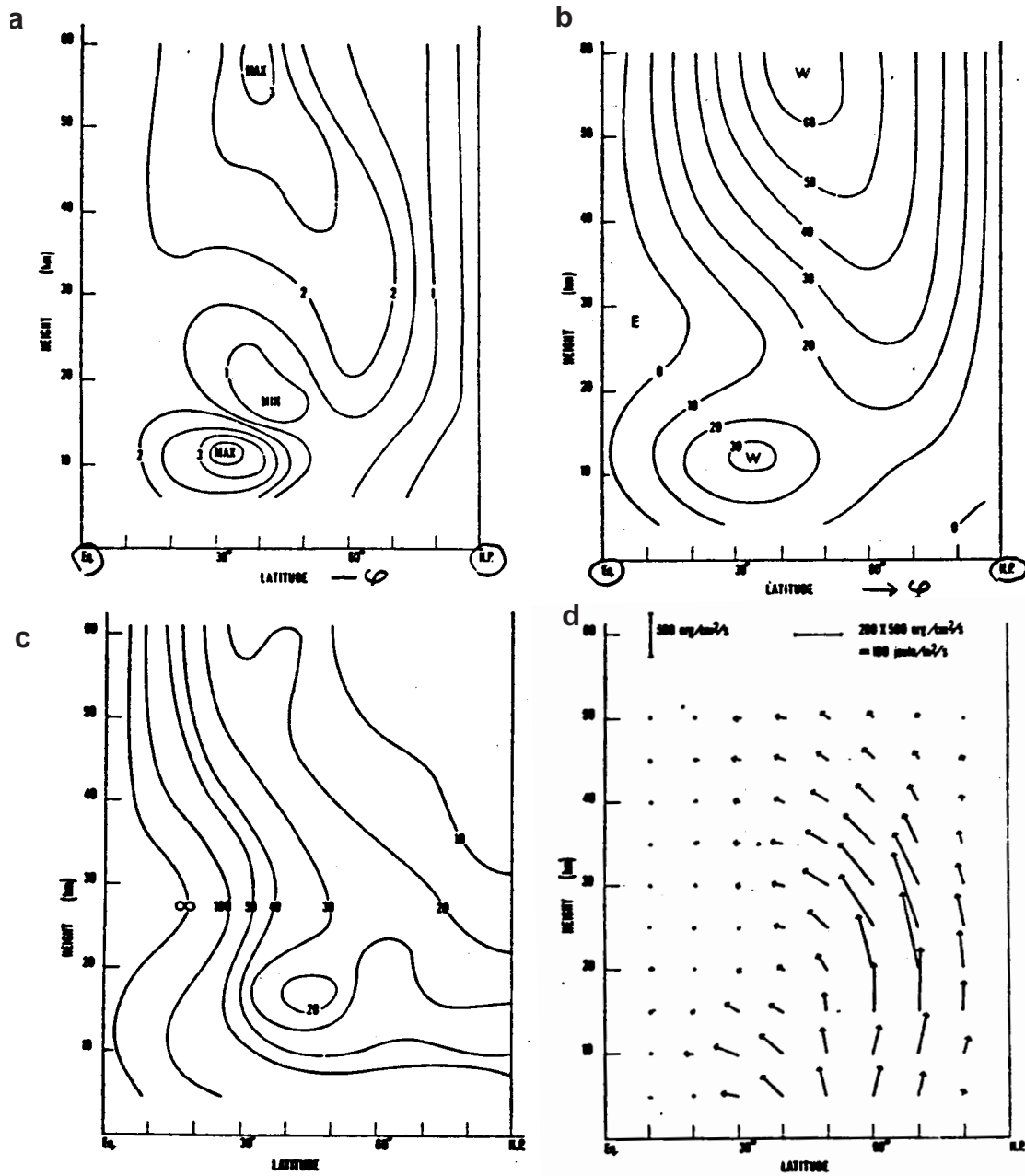


Figure 9.6: a) The latitudinal gradient of the potential vorticity, $\partial[q]/\partial\phi$, expressed as a multiple of the Earth's rotation rate. b) An idealized but somewhat realistic basic state zonal wind distribution (m s^{-1}) in the Northern Hemisphere winter. c) The refractive index square n^2 , for the $k = 0$ wave. d) Computed distribution of energy flow in the meridional plane associated with zonal wave number 1. From Matsuno (1970).

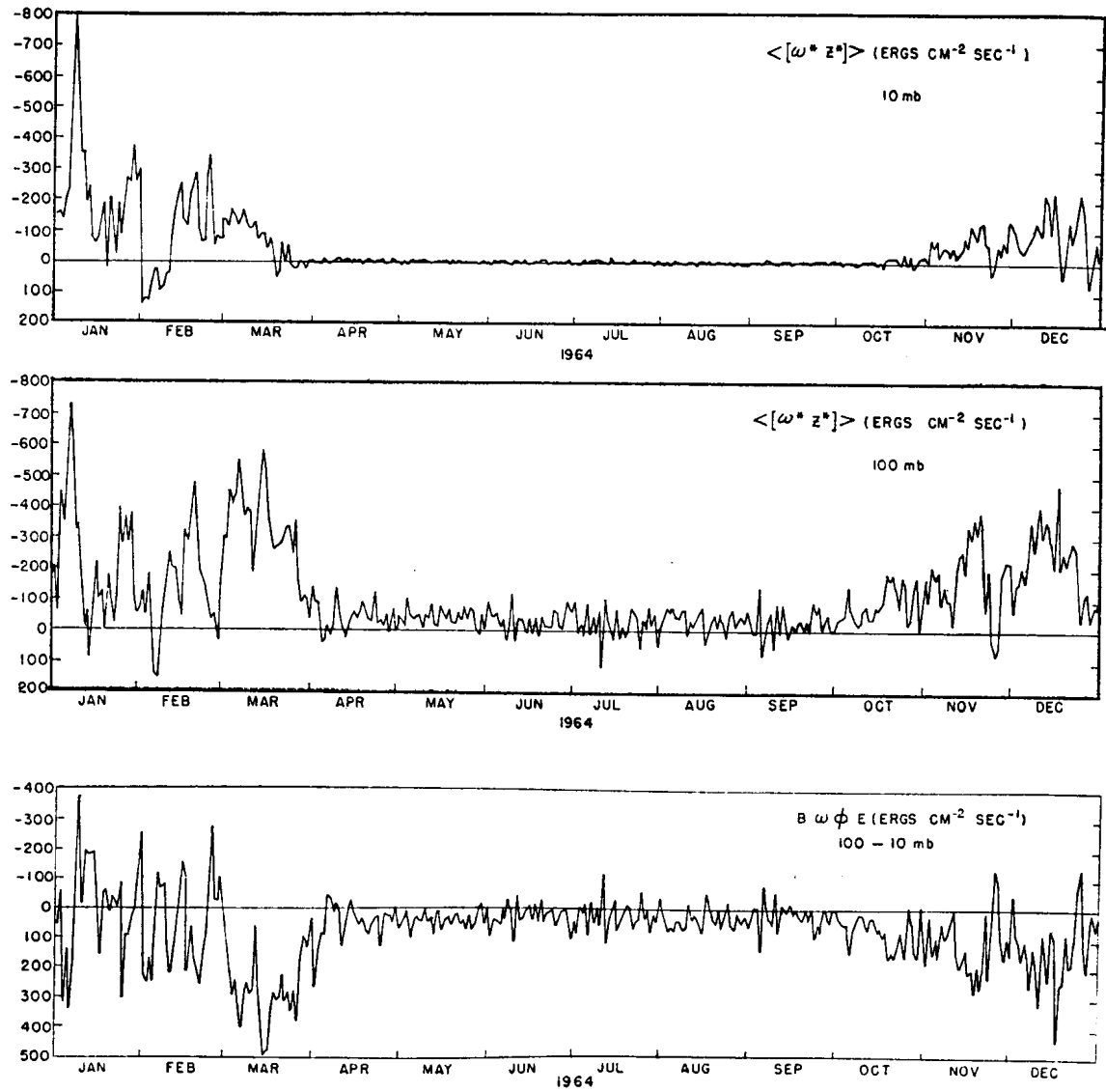


Figure 9.7: a) Daily vertical eddy flux of geopotential through 100 and 10 mb. Units: $\text{erg cm}^{-2} \text{s}^{-1}$. b) Daily divergence of the vertical eddy flux of geopotential for 100-10 mb, and for the region 90°N to 20°N . Units: $\text{erg cm}^{-1} \text{s}^{-1}$. Data for 1964. From Dopplack (1971).

$$\left(\frac{\partial}{\partial t} + [u] \frac{\partial}{\partial x} \right) \psi_z^* - v_* \frac{\partial}{\partial z} [u] + \frac{N^2}{f_0} w^* = 0. \quad (9.41)$$

Here we have used the thermal wind equation. Multiplying (9.41) by ψ_z^* , we obtain a form of the “temperature variance equation:”

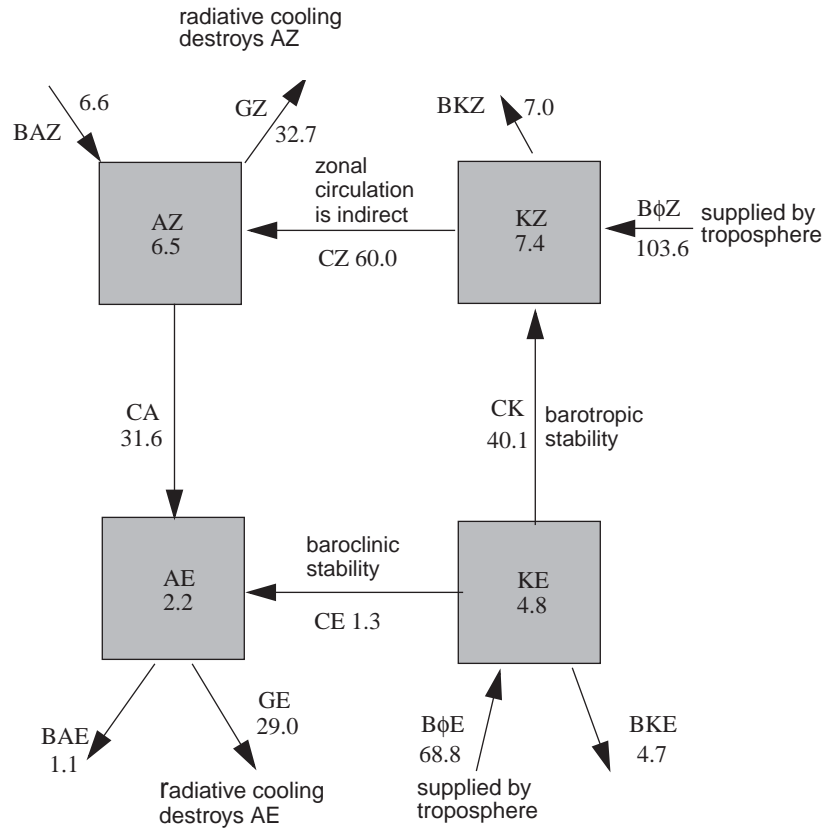


Figure 9.8: Annual energy cycle for the lower stratosphere between 100–10 mb and for the region 20°N to 90°N. Units: contents 10^7 erg cm^{-2} ; conversions: $\text{erg cm}^{-2} \text{ s}^{-1}$. “B” indicates boundary effects (at the lower or equatorward boundaries), and “G” indicates generation. Overall, the stratosphere gains kinetic energy through interactions with the troposphere. The kinetic energy is converted to potential energy. This balances a loss of potential energy through radiative effects. From Doplick (1971).

$$\left(\frac{\partial}{\partial t} + [u] \frac{\partial}{\partial x} \right) \left\{ \frac{1}{2} (\psi_z^*)^2 \right\} - v_* \psi_z^* \frac{\partial [u]}{\partial z} + \frac{N^2}{f_0} w_* \psi_z^* = 0. \quad (9.42)$$

Note the two gradient production terms.

Take [] of (9.42), so that the $[u] \frac{\partial}{\partial x}$ term drops out. Rearrange to isolate the meridional energy flux by itself on the left-hand side:

$$[v_* \psi_z^*] \frac{\partial[u]}{\partial z} = \frac{\partial}{\partial t} \left[\frac{1}{2} (\psi_z^*)^2 \right] + N^2 \left[\frac{w_* \psi_{z*}}{f_0} \right]. \quad (9.43)$$

Note that $[w_* \psi_{z*}]/f_0 > 0$ implies an upward temperature flux, in either hemisphere. Also $[v_* \psi_z^*] > 0$ implies a poleward temperature flux, in either hemisphere.

First, consider a baroclinically *amplifying* wave, for which $\frac{\partial}{\partial t} [(\psi_z^*)^2] > 0$ and the wave temperature flux is upward. From (9.43), we see that such a wave produces a poleward temperature flux (in either hemisphere) when $\frac{\partial[u]}{\partial z} > 0$, i.e. when the temperature is decreasing towards the pole. The heat flux is downgradient, so the gradient-production term is positive.

Next, consider a *neutral* wave of the form $e^{ik(x-ct)}$, for which $\frac{\partial}{\partial t} \psi_z^* = -c \frac{\partial}{\partial x} \psi_z^*$, where c is real. Multiply (9.41) by ψ^* and take the zonal mean, to obtain

$$([u] - c) [v_* \psi_z^*] = N^2 \left[\frac{w_* \psi_{z*}}{f_0} \right]. \quad (9.44)$$

Note that $[w_* \psi_{z*}]/f_0 > 0$ means an upward propagation of wave energy in either hemisphere. Recall also that $[u] - c > 0$ is needed in order for the wave to propagate. It follows that *an upward-propagating neutral wave transports energy poleward*. Such a wave might be forced, for example, by flow over mountains.

In summary, poleward energy transport is produced by *either* a baroclinically amplifying wave with $\frac{\partial[u]}{\partial z} > 0$ *or* a neutral wave that propagates upward.

Applying the eddy PV equation (9.23) to a neutral wave gives

$$([u] - c) \frac{\partial q_*}{\partial x} + v_* \frac{\partial [q]}{\partial y} = 0. \quad (9.45)$$

Multiply (9.45) by ψ_* and take the zonal mean to show that

$$[v_* q_*] = 0 \text{ except where } [u] = c \quad (9.46)$$

(the critical level). This very important result shows that neutral waves produce no potential vorticity flux except at a critical level. It follows from (9.16) that *neutral waves do not affect $[q]$ except at a critical level*. This is a non-interaction theorem for planetary waves, analogous to the result obtained for gravity waves by Eliassen and Palm (1961).

From (9.17), $[v_* q_*] = 0$ means

$$-\frac{\partial}{\partial y}[u_* v_*] + \frac{f_0^2}{\rho_S} \frac{\partial}{\partial z} \left(\frac{\rho_S}{N^2} [v_* \psi_z^*] \right) = 0. \quad (9.47)$$

As we will see later, the expression equal to zero in (9.47) is the divergence of the Eliassen-Palm flux.

Vertically integrate (9.47) through the depth of the atmosphere to obtain

$$-\int_0^{p_S} \frac{\partial}{\partial y} [u_* v_*] \frac{dp}{g} = f_0^2 \frac{\rho_S}{N^2} [v_* \psi_z^*]_S. \quad (9.48)$$

for the neutral waves. The left-hand side represents the vertically integrated convergence of meridional momentum flux, and the right-hand side represents the near-surface value of the eddy meridional energy flux. Recall from (9.44) that an upward propagating neutral wave produces a poleward energy flux, i.e. $[v_* \psi_z^*] > 0$. It follows from (9.48) that

$$-\int_0^{p_S} \frac{\partial}{\partial y} [u_* v_*] \frac{dp}{g} > 0. \quad (9.49)$$

This means that the vertically integrated meridional momentum flux divergence tends to accelerate the vertically integrated $[u]$. In other words, the eddies feed the jet! This explains why we observe $KE \rightarrow KZ$. If the waves are also transporting temperature poleward, they will tend to reduce the meridional temperature gradient and so tend to reduce the strength of the westerlies. The momentum flux and heat flux thus have opposing effects on the mean flow.

An upward propagating neutral wave in westerly shear tends to produce a downward momentum flux at the Earth's surface. To see this, consider the zonal momentum equation, in Cartesian coordinates for simplicity:

$$\frac{\partial u}{\partial t} + \frac{\partial}{\partial x}(uu) + \frac{\partial}{\partial y}(uv) + \frac{1}{\rho_S} \frac{\partial}{\partial z}(\rho_S u w) = -\frac{\partial \phi}{\partial x} + f v. \quad (9.50)$$

We have neglected the metric term and assumed no friction above the boundary layer. Taking the zonal mean of (9.50) gives

$$\frac{\partial [u]}{\partial t} + \frac{\partial}{\partial y} [u^* v^*] + \frac{1}{\rho_S} \frac{\partial}{\partial z} (\rho_S [u^* w^*]) = f [v]. \quad (9.51)$$

Here advection of $[u]$ by $[v]$ and $[w]$ is neglected; this is justified in the midlatitude winter. To

the extent that $[v]$ is geostrophic, it vanishes anyway. Now assume $\frac{\partial[u]}{\partial t} = 0$, consistent with $\frac{\partial[q]}{\partial t} = 0$. This leads to

$$\frac{\partial}{\partial y}[u^* v^*] = -\frac{1}{\rho_S} \frac{\partial}{\partial z}(\rho_S[u^* w^*]) + f[v] . \quad (9.52)$$

Integrating (9.52) vertically with respect to mass, using $\int_0^\infty \rho_S[v] dz \cong 0$, and employing (9.49), we find that

$$\int_0^\infty \frac{\partial}{\partial z}(\rho_S[u_* w_*]) dz > 0 . \quad (9.53)$$

We know that $\rho_S[u_* w_*]$ must vanish at great height, so we conclude that

$$\rho_S[u_* w_*]_S < 0 . \quad (9.54)$$

This shows that, near the lower boundary, friction and/or mountain torque must carry westerly momentum into the Earth's surface, in the presence of an upward propagating planetary wave. An alternative interpretation is that frictional and/or mountain torque, in a belt of westerlies where (9.54) is satisfied, will produce an upward-propagating planetary wave that transports energy poleward.

Compare (9.49) and (9.54). The meridional momentum flux accelerates the westerlies, while the vertical momentum flux decelerates them.

9.4 Sudden warmings

The preceding discussion is highly relevant to stratospheric sudden warmings. This is how stratospheric sudden warmings work: The polar stratosphere is observed to warm up, while the lower latitudes cool off, as shown in the upper panel of Fig. 9.9. There is no significant change of the *area-averaged* temperature, however. This suggests that the sudden warming is due to a poleward redistribution of sensible heat. The polar westerlies are observed to weaken, and in some cases they give way to easterlies. There are two mechanisms that can change the zonally averaged temperature by meridional redistribution of sensible heat. The possibilities are:

- *A mean meridional circulation.* Sinking near the poles can produce adiabatic warming, while the compensating rising motion in lower latitudes gives adiabatic cooling. This MMC would be *direct*, at least to start with.
- *Poleward eddy energy transport.* In this case, eddies produce warming near the pole and cooling in lower latitudes. An MMC would be produced by the

“apparent” heating and cooling due to the eddies. This MMC would feature rising at the pole to counteract the eddy warming there, and sinking in lower latitudes to counteract the eddy cooling there. This means that the MMC would be *indirect*.

In the first scenario, the westerlies will increase aloft. (Why?) Since the westerly shear must decrease during a sudden warming (Why?), there must be an even stronger intensification of the westerlies below. In the second scenario, on the other hand, the westerlies will weaken above. *The observed transition to easterlies in the stratosphere supports the second hypothesis.* We conclude that stratospheric sudden warmings are produced by poleward eddy heat fluxes.

Sudden warmings are characterized by intense wave activity, of planetary scale. The longitudinal phase is stationary, suggesting orographic forcing. Sudden warmings are relatively infrequent and weak in the Southern Hemisphere, where there is little orography.

There is a strong flux of wave energy from the troposphere to the stratosphere during winter. From our previous analysis, we know that such a wave will transport energy poleward. A sudden warming is triggered by the rapid growth of a quasistationary planetary wave in the troposphere, and its subsequent upward propagation into the stratosphere. As shown in Fig. 9.9 and Fig. 9.10, there is observational evidence for such wave growth, often in association with the formation of a blocking high (discussed later).

As it propagates upward, the planetary wave transports energy poleward and so weakens the westerlies aloft. In extreme cases, the westerlies are actually changed to easterlies. When easterlies form above, the wave propagation is blocked, so the wave energy is concentrated near the critical level. This leads to *really* sudden warming.

Matsuno (1971) was the first to successfully simulate sudden warmings with a numerical model.

9.5 *Eliassen-Palm Theorem-Reprise*

Previously we discussed non-interaction theorems for pure gravity waves and for quasi-geostrophic waves on a β -plane. It was discovered during the 1970's that non-interaction theorems can be derived for very general balanced flows. The following discussion provides an example. The discussion is based on Andrews et al. (1987).

The zonally averaged momentum equations in spherical coordinates can be written as

$$\begin{aligned} \frac{\partial[u]}{\partial t} + [v] \left\{ \frac{1}{a \cos \varphi} \left(\cos \varphi \frac{\partial[u]}{\partial \varphi} - [u] \sin \varphi \right) - f \right\} + [w] \frac{\partial[u]}{\partial z} - [F_x] \\ = \frac{-1}{a \cos^2 \varphi} \frac{\partial}{\partial \varphi} ([u_* v_*] \cos^2 \varphi) - \frac{1}{\rho_s} \frac{\partial}{\partial z} (\rho_s [u_* w_*]) , \end{aligned} \quad (9.55)$$

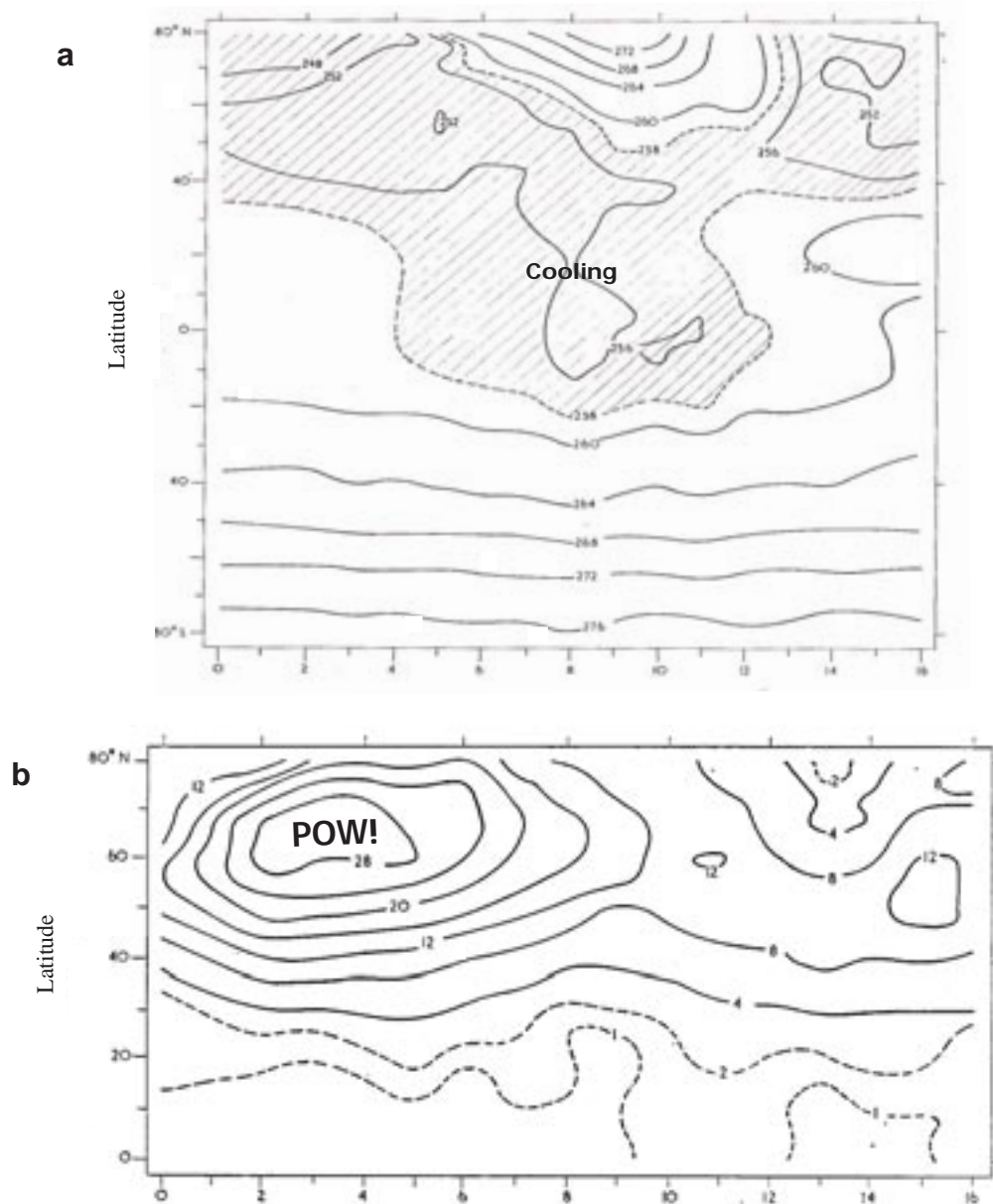
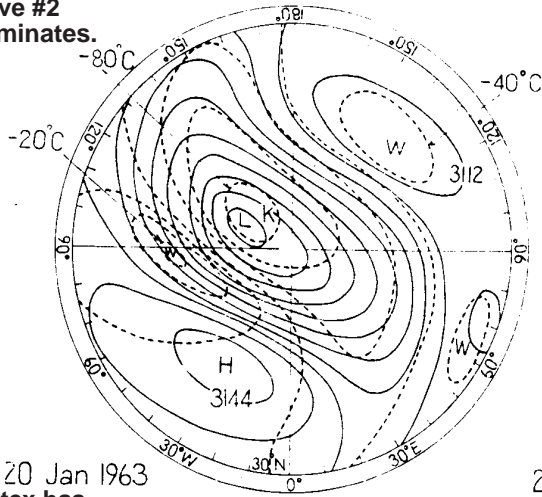
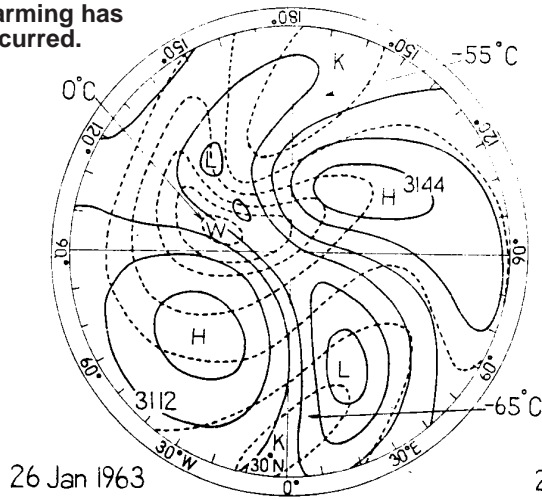


Figure 9.9: a) Latitude-time section of zonal mean temperature (K) measured by channel A for 31 December 1970 to 16 January 1971. Regions of temperature lower than 258 K are shaded. A major warming had a peak at this level on 9 January at 80°N. b) Latitude-time section of amplitude of zonal wavenumber one of channel A temperature (K) for 31 December 1970 to 16 January 1971. Maximum amplitude occurred on 4 January at 65°N. From Barnett (1974).

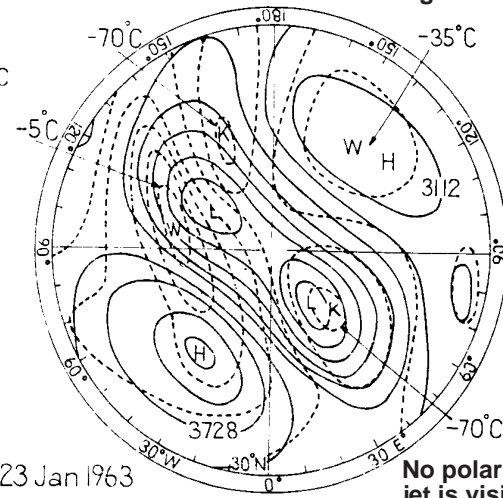
Westerlies with
a polar vortex.
Wave #2
dominates.



20 Jan 1963
Vortex has
broken.
Warming has
occurred.



Vortex has
become
elongated.



No polar night
jet is visible.
Easterlies
prevail.

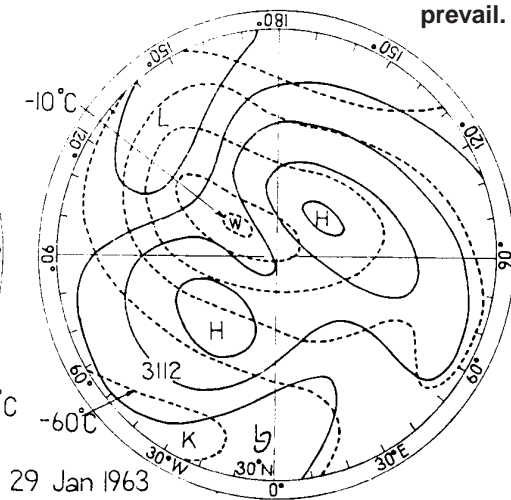


Figure 9.10: 10 mb charts during a sudden warming in January 1963. Height contours (solid lines) at 32 dm intervals. Isotherms (dashed lines) at 10 K intervals. Note that the process spans 9 days. From Sawyer (1965).

$$\begin{aligned}
 & \frac{\partial[v]}{\partial t} + \frac{1}{a}[v] \frac{\partial[v]}{\partial \phi} + [w] \frac{\partial[v]}{\partial z} + [u] \left(f + \frac{[u] \tan \phi}{a} \right) + \frac{1}{a} \frac{\partial[\phi]}{\partial \phi} - [F_y] \\
 & = \frac{-1}{a \cos \phi} \frac{\partial}{\partial \phi} ([v_*^2] \cos \phi) - \frac{1}{\rho_S} \frac{\partial}{\partial z} (\rho_S [v_* w_*]) - \frac{[u_*^2] \tan \phi}{a}.
 \end{aligned}
 \tag{9.56}$$

Here $z \equiv -H \log(p/p_S)$ is the vertical coordinate, and $w \equiv Dz/Dt$. The scale height H is $\frac{RT_0}{g}$, where T_0 is a constant. The zonally averaged thermodynamic energy equation is

$$\begin{aligned} & \frac{\partial[\theta]}{\partial t} + \frac{1}{a} [v] \frac{\partial[\theta]}{\partial \varphi} + [w] \frac{\partial[\theta]}{\partial z} - [Q] \\ &= \frac{-1}{a \cos \varphi} \frac{\partial}{\partial \varphi} ([\theta^* v^*] \cos \varphi) - \frac{1}{\rho_S} \frac{\partial}{\partial z} (\rho_S [w^* \theta^*]) . \end{aligned} \quad (9.57)$$

Here Q represents a heating process. Finally, we will need the zonally averaged continuity equation,

$$\frac{1}{a \cos \varphi} \frac{\partial}{\partial \varphi} (\rho_S [v] \cos \varphi) + \frac{\partial}{\partial z} (\rho_S [w]) = 0 , \quad (9.58)$$

and hydrostatics:

$$\frac{\partial[\phi]}{\partial z} - \frac{R[\theta]}{H} e^{-\frac{Kz}{H}} = 0 . \quad (9.59)$$

In the above equations, $\rho_S(z) \equiv \rho_0 e^{-\frac{z}{H}}$, where ρ_0 is a constant. We assume that (9.56) can be approximated by *gradient wind balance*, i.e.

$$[u] \left(f + [u] \frac{\tan \varphi}{a} \right) + \frac{1}{a} \frac{\partial[\phi]}{\partial \varphi} = 0 . \quad (9.60)$$

This assumed balance is essential to the following argument.

We define a “residual mean meridional circulation” ($0, V, W$) by

$$V \equiv [v] - \frac{1}{\rho_S} \frac{\partial}{\partial z} \left(\frac{\rho_S [v^* \theta^*]}{\frac{\partial[\theta]}{\partial z}} \right) , \quad (9.61)$$

$$W \equiv [w] + \frac{1}{a \cos \varphi} \frac{\partial}{\partial \varphi} \left(\cos \varphi \frac{[v^* \theta^*]}{\frac{\partial[\theta]}{\partial z}} \right) . \quad (9.62)$$

In the absence of eddies, $V = [v]$ and $W = [w]$. Substitution shows that V and W satisfy a continuity equation analogous to (9.58). Use of (9.61) and (9.62) to eliminate $[v]$ and $[w]$ in favor of V and W allows us to rewrite (9.55) and (9.57) as:

$$\frac{\partial[u]}{\partial t} + V \left\{ \frac{1}{a \cos \varphi} \frac{\partial}{\partial \varphi} ([u] \cos \varphi) - f \right\} + W \frac{\partial[u]}{\partial z} - [F_x] = \frac{1}{\rho_S a \cos \varphi} (\nabla \cdot \mathbf{EPF}) \quad (9.63)$$

and

$$\begin{aligned} \frac{\partial[\theta]}{\partial t} + \frac{V}{a} \frac{\partial[\theta]}{\partial \varphi} + W \frac{\partial[\theta]}{\partial z} - [Q] = \\ \frac{-1}{\rho_S} \frac{\partial}{\partial z} \left\{ \left(\frac{\partial[\theta]}{\partial z} \right)^{-1} \rho_S [v^* \theta^*] \frac{1}{a} \frac{\partial[\theta]}{\partial \varphi} + \rho_S [w^* \theta^*] \right\}, \end{aligned} \quad (9.64)$$

respectively where

$$\mathbf{EPF} \equiv [0, (EPF)_\varphi, (EPF)_z] \quad (9.65)$$

is the ‘‘Eliassen-Palm flux,’’ whose components are

$$(EPF)_\varphi \equiv \rho_S a \cos \varphi \left\{ \frac{\partial[u]}{\partial z} \cdot \frac{[v^* \theta^*]}{\frac{\partial[\theta]}{\partial z}} - [u^* v^*] \right\}, \quad (9.66)$$

and

$$(EPF)_z \equiv \rho_S a \cos \varphi \left\{ \left\{ f - \frac{1}{a \cos \varphi} \frac{\partial}{\partial \varphi} ([u] \cos \varphi) \right\} \frac{[v^* \theta^*]}{\frac{\partial[\theta]}{\partial z}} - [u^* w^*] \right\}. \quad (9.67)$$

In (9.66), the $-[v^* u^*]$ term is dominant, and in (9.67) the $[v^* \theta^*]$ term is dominant. Compare (9.66) and (9.67) with (9.17) and (9.47). When the \mathbf{EPF} points upward, the meridional energy flux is in control. When it points in the meridional direction, the meridional flux of zonal momentum is in control. From (9.63) we see that a positive Eliassen-Palm flux divergence tends to increase $[u]$.

The preceding derivation appears to be nothing more than an algebraic shuffle. We wrote down (9.61) and (9.62) without any explanation or motivation. What is the point of all this? The point is that for steady linear waves with $F_x = F_y = 0$ and $Q = 0$, it can be shown that

$$\nabla \bullet (\mathbf{EPF}) = 0. \quad (9.68)$$

Recall that this follows essentially from $[v_* q_*] = 0$. It turns out that the eddy forcing term of (9.64) is zero under the same conditions, i.e.

$$\frac{1}{\rho_S} \frac{\partial}{\partial z} \left\{ \left(\frac{\partial [\theta]}{\partial z} \right)^{-1} \rho_S [v^* \theta^*] \frac{1}{a} \frac{\partial [\theta]}{\partial \phi} + \rho_S [w^* \theta^*] \right\} = 0. \quad (9.69)$$

This follows essentially from the facts that: 1) $[u]$ does not change, and 2) thermal wind balance is maintained.

For the case of steady, linear waves, in the absence of friction and heating, our system of equations reduces to

$$\begin{aligned} \frac{\partial [u]}{\partial t} + V \left\{ \frac{1}{a \cos \phi} \frac{\partial}{\partial \phi} ([u] \cos \phi) - f \right\} + W \frac{\partial [u]}{\partial z} &= 0, \\ [u] \left(f + [u] \frac{\tan \phi}{a} \right) + \frac{1}{a} \frac{\partial [\phi]}{\partial \phi} &= 0, \\ \frac{\partial [\theta]}{\partial t} + \frac{V}{a} \frac{\partial [\theta]}{\partial \phi} + W \frac{\partial [\theta]}{\partial z} &= 0, \\ \frac{1}{a \cos \phi} \frac{\partial}{\partial \phi} (\rho_S V \cos \phi) + \frac{\partial}{\partial z} \rho_S W &= 0, \\ \frac{\partial [\phi]}{\partial z} - H^{-1} R [\theta] e^{-\frac{\kappa z}{H}} &= 0. \end{aligned} \quad (9.70)$$

This system has the following steady solution:

$$\begin{aligned} \frac{\partial [u]}{\partial t} &= 0, u \text{ in gradient - wind balance,} \\ V &= 0, \\ W &= 0, \\ \frac{\partial [\theta]}{\partial t} &= 0, [\theta] \text{ given externally (e.g., initial values or radiative-convective equilibrium).} \end{aligned} \quad (9.71)$$

This is essentially the same solution that we discussed in Chapter 4. (There $[\theta]$ was determined by θ_E .) From the definitions of V and W , we can find the mean meridional circulation implied by $V = 0$ and $W = 0$:

$$\rho_S[v] = \frac{\partial}{\partial z} \left(\rho_S \frac{[v^* \theta^*]}{\frac{\partial[\theta]}{\partial z}} \right), \quad (9.72)$$

$$[w] = -\frac{1}{a \cos \varphi} \frac{\partial}{\partial \varphi} \left(\cos \varphi \frac{[v^* \theta^*]}{\frac{\partial[\theta]}{\partial z}} \right). \quad (9.73)$$

Suppose we have a solution with *no eddies* at all. “No eddies” certainly qualify as “steady linear waves.” The above argument therefore applies, so we can get $[u]$, $[\theta]$, and from (9.72) and (9.73) we conclude that the MMC will vanish. This is essentially the same solution that we discussed in Chapter 4, for the case of no friction.

Now add steady linear eddies, so that $\nabla \bullet (\mathbf{EPF})$ continues to be zero. Then *exactly the same* $[u]$ and $[\theta]$ will satisfy the equations! Of course, $[v]$ and $[w]$ will be different, i.e., the MMC will be different. The MMC will in fact have to be just what it takes to ensure that $V = W = 0$, i.e. to satisfy (9.72) and (9.73). We can say that this MMC is “induced by” the eddies. The system produces this MMC in order to prevent the eddies from disrupting the thermal wind balance. Perhaps a better way to say this is that the processes that act to maintain thermal wind balance (i.e. geostrophic and hydrostatic adjustment) accomplish this feat by using the “wave-induced” MMC as a tool.

The interpretation of this amazing result is that if you try to modify $[u]$ and $[\theta]$ by applying eddy forcing such that $\nabla \bullet (\mathbf{EPF}) = 0$ (no potential vorticity flux), you will be disappointed! All that will happen is that the MMC will change, in such a way that V and W continue to be zero. In effect, *the eddies will induce an MMC that exactly cancels the direct effects of the eddies on* $[u]$ and $[\theta]$.

When the eddies are unsteady, the residual circulation is different from zero, and $[u]$ and $[\theta]$ are modified by the combined effects of the eddies and/or the eddy-induced MMC. Cancellation of the effects of the eddies and the MMC still tends to occur, but the cancellation is incomplete.

Edmon et al. (1980) discussed the quasi-geostrophic form of the non-interaction theorem, and used it to analyze the data of Oort and Rasmussen (1971). As a reminder [see (9.47)], the meridional component of the quasigeostrophic *EPF* is

$$(EPF)_\varphi = -a \cos(\varphi) [\overline{u^* v^*}] , \quad (9.74)$$

and the vertical component is

$$(EPF)_p = fa \cos(\varphi) \frac{[\overline{v^* \theta^*}]}{\frac{\partial \bar{\theta}}{\partial p}} . \quad (9.75)$$

[Note: Compare (9.74) and (9.75) with (9.66) and (9.67), respectively.] Fig. 9.11 shows the

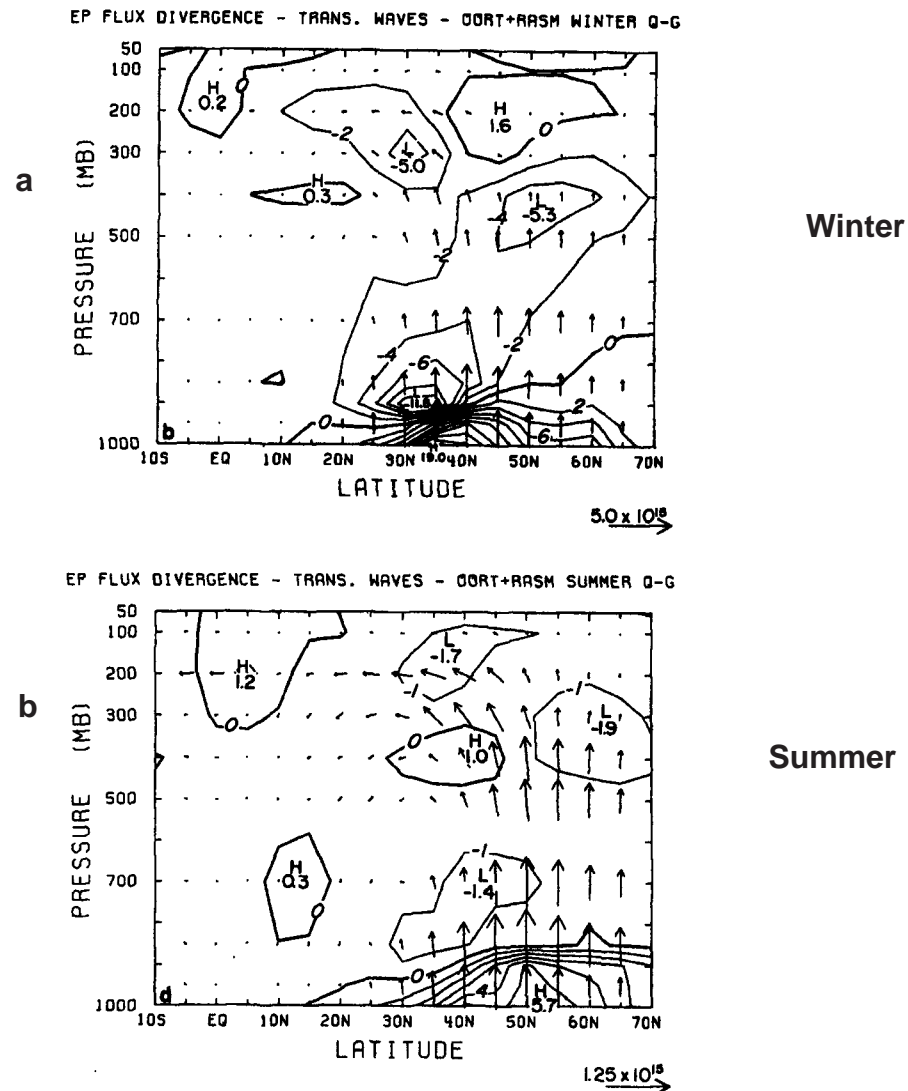


Figure 9.11: Contribution of *transient* eddies to the seasonally averaged Eliassen-Palm cross sections for the troposphere: (a) 5-year average from Oort and Rasmusson (1971) for winter; (b) the same for summer. The contour interval is $20 \times 10^{15} \text{ m}^3$ for (a), and $1 \times 10^{15} \text{ m}^3$ for (b). The horizontal arrow scale for the horizontal component in units of m^3 is indicated at bottom right; note that it is different from diagram to diagram. A vertical arrow of the same length represents the vertical component, in $\text{m}^3 \text{ kPa}$, equal to that for the horizontal arrow multiplied by 80.4 kPa. From Edmon et al. (1980).

contribution of the transient eddies to the Eliassen-Palm fluxes. First consider the winter results, shown in the upper panel. Near the surface in middle latitudes, we see arrows pointing strongly upward, indicating an intense poleward potential temperature flux. Near the tropopause, the arrows curve over and become horizontal, pointing towards the tropics. This indicates a strong poleward eddy momentum flux. The contours in the figure show the

divergence of the Eliassen-Palm flux. Keep in mind that $\nabla \bullet (\mathbf{EPF} > 0 \text{ means } \frac{\partial[u]}{\partial t} > 0)$, i.e. a positive **EPF** divergence favors westerly acceleration. The negative divergence (i.e. convergence) near 200 mb at about 30° N indicates that the *net effect* of the eddies is to decelerate the jet. In fact, the westerlies are being decelerated throughout middle latitudes, except near the surface. Note that this **EPF** convergence results mainly from the upward decrease of the upward component of the flux, i.e. it is mainly due to the energy flux.

The results for summer are quite similar, except that everything is weaker, and shifted poleward.

Fig. 9.12 shows the corresponding results for the stationary waves. In winter, the “strong” arrows are pointing nearly straight up everywhere, indicating that the poleward eddy potential temperature flux is playing a much more important role than the eddy momentum flux. The westerlies are decelerated aloft, near 50° N, but they are accelerated near the surface. In summer the arrows point downward. The eddy momentum flux is important near the summer tropopause, but again the eddy potential temperature flux is more important overall. The westerlies are strongly decelerated near the surface in the subtropics, and they are actually accelerated at 200 mb near 35° N.

Fig. 9.13 shows the combined effects of the transient and stationary eddies. Note that the transient eddies dominate, in both seasons. Finally, Fig. 9.14 shows the residual circulation, (V, W) , for summer and winter. In winter, the residual circulation looks suspiciously like a giant Hadley Cell, extending from the tropics to the poles. This is reminiscent of the mean meridional circulation as seen in isentropic coordinates. In summer, we seem to see the northern edge of a Hadley Cell extending into the Southern Hemisphere. Clearly, we can regard the residual circulation as a response to heating.

9.6 The Eliassen-Palm theorem in isentropic coordinates

The Eliassen-Palm theorem is somewhat simpler and easier to interpret when we use isentropic coordinates. Following Andrews (1983), we begin with the flux form of the zonal momentum equation with an isentropic coordinate, neglecting body forces:

$$\begin{aligned} \frac{\partial}{\partial t}(mu) + \frac{1}{a \cos \phi} \left[\frac{\partial}{\partial \lambda}(muu) + \frac{\partial}{\partial \phi}(mu v \cos \phi) \right] - mv \left(f + \frac{u \tan \phi}{a} \right) \\ = - \frac{m}{a \cos \phi} \frac{\partial M}{\partial \lambda} - \frac{\partial}{\partial \theta}(mu \dot{\theta}) . \end{aligned} \quad (9.76)$$

Here m is the pseudo-density:

$$m = -\frac{1}{g} \frac{\partial p}{\partial \theta}, \quad (9.77)$$

and M is the Montgomery potential:

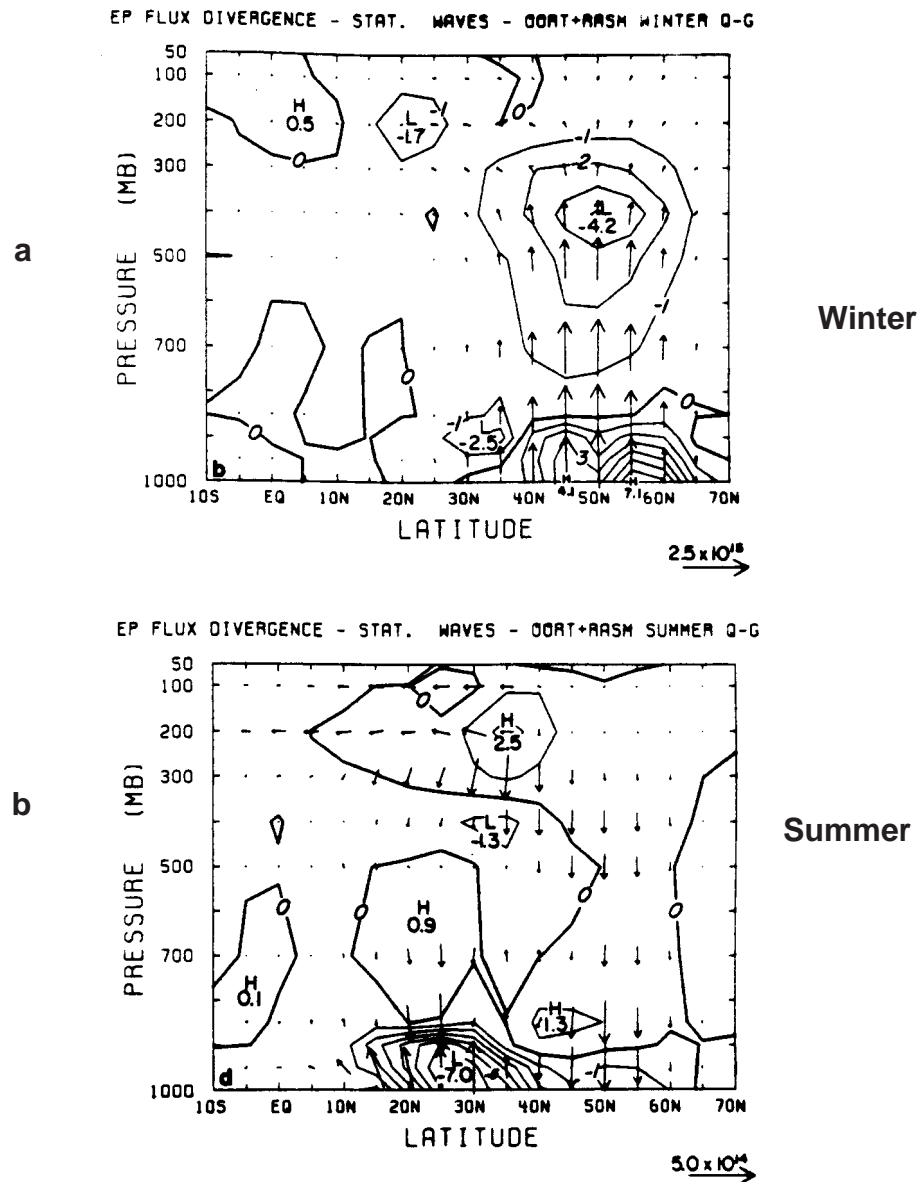


Figure 9.12: Contribution of *stationary* eddies to the seasonally averaged Eliassen-Palm cross sections for the troposphere: (a) 5-year average from Oort and Rasmusson (1971) for winter; (b) the same, respectively, for summer. The contour interval is $1 \times 10^{15} \text{ m}^3$ for both panels. The horizontal arrow scale in units of m^3 is indicated at bottom right. From Edmon et al. (1980).

$$\begin{aligned} M &= c_p T + gz \\ &= \Pi \theta + gz \quad , \end{aligned} \tag{9.78}$$

where

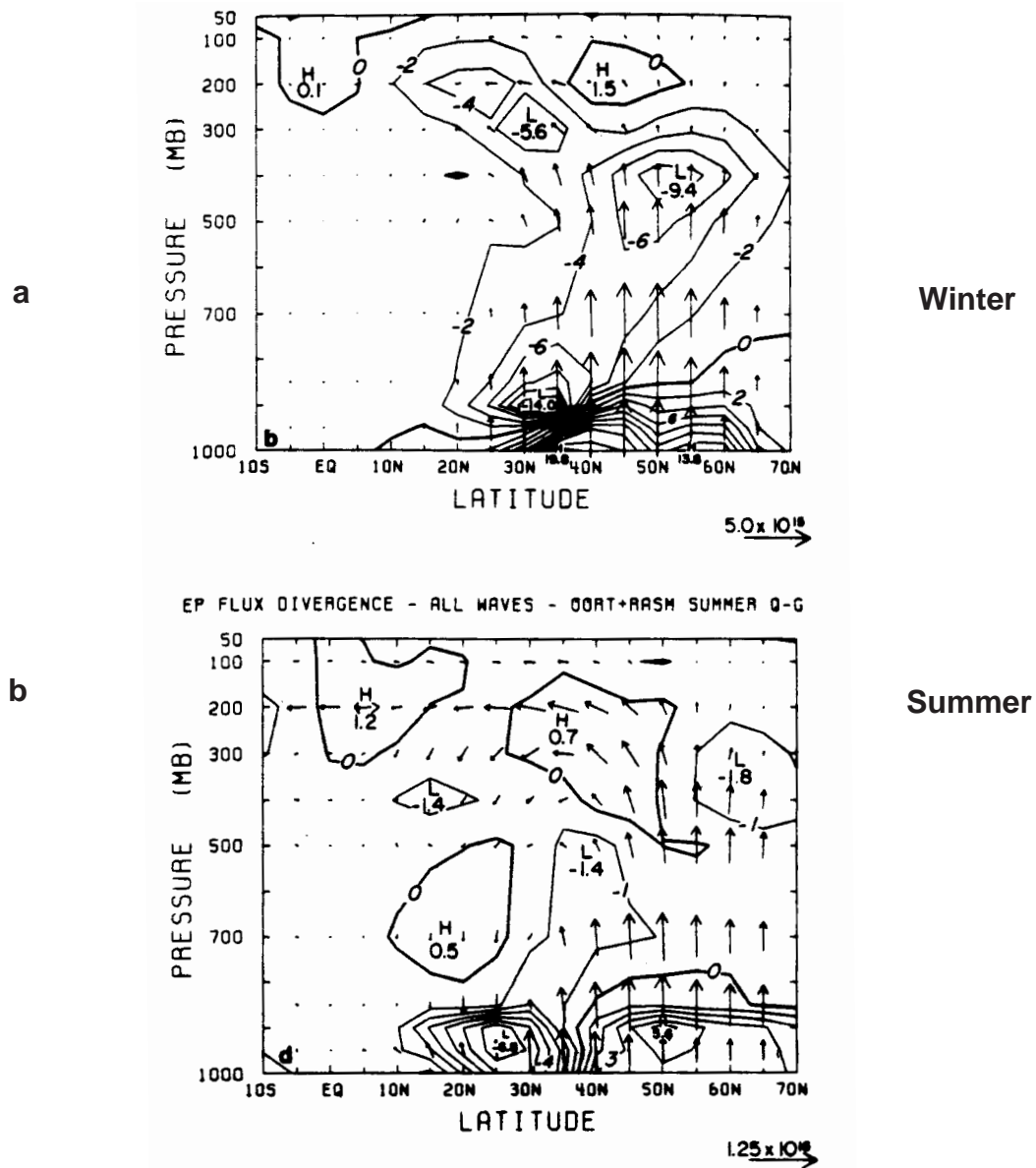


Figure 9.13: Total (transient plus stationary) Eliassen-Palm cross sections for the troposphere: (a) 5-year average from Oort and Rasmusson (1971) for winter; (b) the same, respectively, for summer. The contour interval is $2 \times 10^{15} \text{ m}^3$ for (a), and $1 \times 10^{15} \text{ m}^3$ for (b). The horizontal arrow scale in units of m^3 is indicated at bottom right. From Edmon et al. (1980).

$$\Pi \equiv c_p \left(\frac{p}{p_0} \right)^\kappa. \quad (9.79)$$

We can write

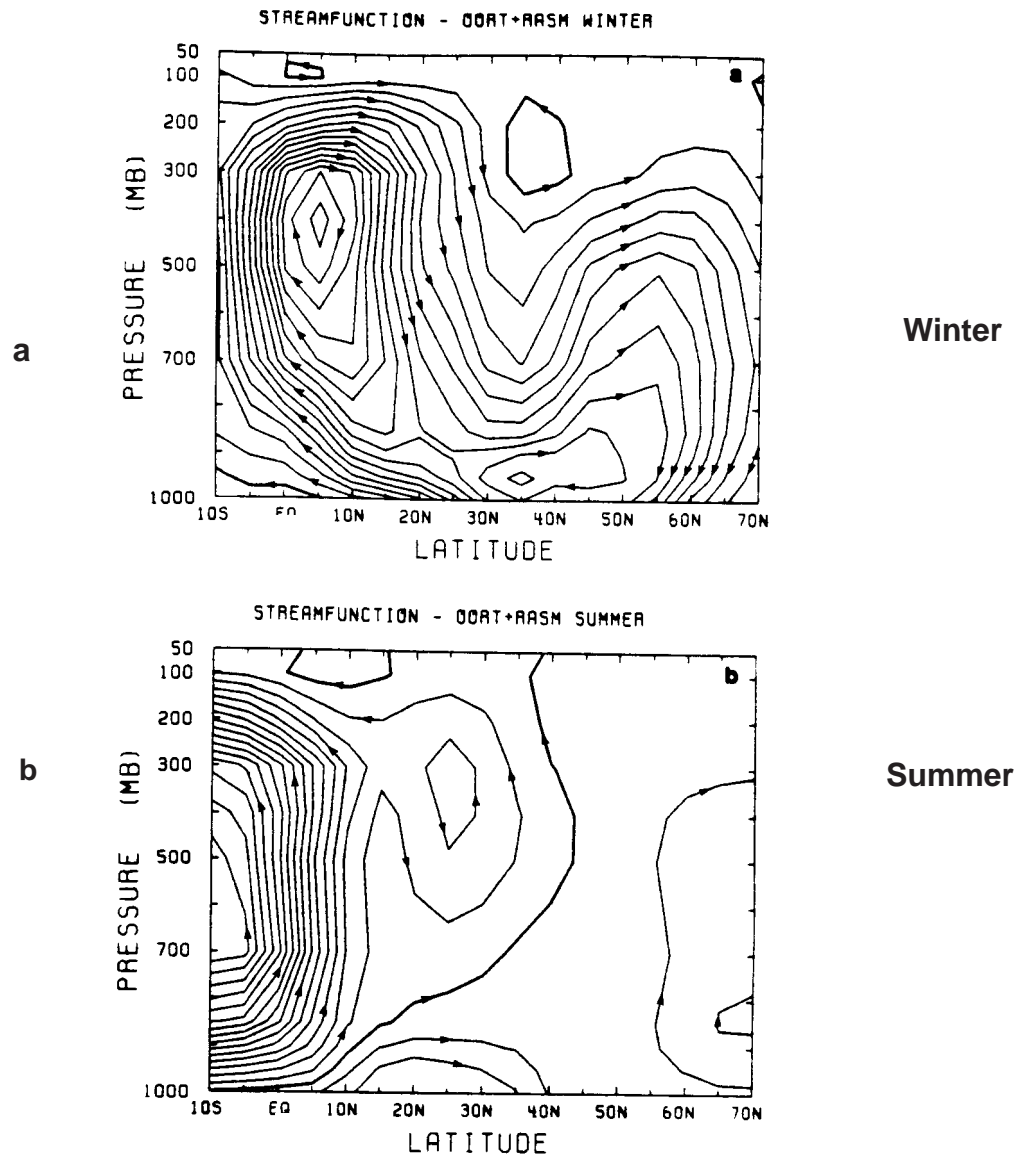


Figure 9.14: The stream function of the seasonally averaged residual meridional circulations. (a) 5-year average from Oort and Rasmusson (1971) for winter, and (b) the same for summer. The contour interval is $7.5 \times 10^{16} \text{ m}^2 \text{ s Pa}$. From Edmon et al. (1980).

Using the hydrostatic equation in isentropic coordinates, i.e.,

$$\frac{\partial M}{\partial \theta} = \Pi, \quad (9.80)$$

we obtain

$$\begin{aligned}
m \frac{\partial M}{\partial \lambda} &= -\frac{1}{g} \frac{\partial p}{\partial \theta} \frac{\partial M}{\partial \lambda} \\
&= -\frac{1}{g} \frac{\partial}{\partial \theta} \left(p \frac{\partial M}{\partial \lambda} \right) + \frac{p}{g} \frac{\partial}{\partial \lambda} \left(\frac{\partial M}{\partial \theta} \right) \\
&= -\frac{1}{g} \frac{\partial}{\partial \theta} \left\{ p \frac{\partial}{\partial \lambda} (\Pi \theta + gz) \right\} + \frac{p}{g} \frac{\partial \Pi}{\partial \lambda} \\
&= -\frac{\partial}{\partial \theta} \left(\frac{\theta p}{g} \frac{\partial \Pi}{\partial \lambda} + p \frac{\partial z}{\partial \lambda} \right) + \frac{p}{g} \frac{\partial \Pi}{\partial \lambda} \\
&= -\frac{\partial}{\partial \theta} \left(\frac{\theta p}{g} \frac{\partial \Pi}{\partial \lambda} \right) + \frac{p}{g} \frac{\partial \Pi}{\partial \lambda} - \frac{\partial}{\partial \theta} \left(p \frac{\partial z}{\partial \lambda} \right) \\
&= -\theta \frac{\partial}{\partial \theta} \left(\frac{p}{g} \frac{\partial \Pi}{\partial \lambda} \right) - \frac{\partial}{\partial \theta} \left(p \frac{\partial z}{\partial \lambda} \right).
\end{aligned} \tag{9.81}$$

Substituting back, the momentum equation becomes

$$\begin{aligned}
\frac{\partial}{\partial t}(mu) + \frac{1}{a \cos \varphi} \left\{ \frac{\partial}{\partial \lambda}(muu) + \frac{\partial}{\partial \varphi}(muv \cos \varphi) \right\} - mv \left(f + \frac{u \tan \varphi}{a} \right) \\
= \frac{1}{a \cos \varphi} \left\{ \theta \frac{\partial}{\partial \theta} \left(\frac{p}{g} \frac{\partial \Pi}{\partial \lambda} \right) + \frac{\partial}{\partial \theta} \left(p \frac{\partial z}{\partial \lambda} \right) \right\} - \frac{\partial}{\partial \theta}(mu\dot{\theta}).
\end{aligned} \tag{9.82}$$

When we take the zonal mean of (9.82), we get

$$\begin{aligned}
\frac{\partial}{\partial t}[mu] + \frac{1}{a \cos \varphi} \left\{ \frac{\partial}{\partial \varphi}([muv] \cos \varphi) \right\} - \left([mv]f + \frac{[mvu] \tan \varphi}{a} \right) \\
= \frac{1}{a \cos \varphi} \frac{\partial}{\partial \theta} \left[p^* \frac{\partial z}{\partial \lambda} \right] - \frac{\partial}{\partial \theta}[mu\dot{\theta}].
\end{aligned} \tag{9.83}$$

This can be simplified slightly by combining the second and fourth terms:

$$\begin{aligned}
\frac{\partial}{\partial t}[mu] + \frac{1}{a \cos^2 \varphi} \left\{ \frac{\partial}{\partial \varphi}([muv] \cos^2 \varphi) \right\} - [mv]f \\
= \frac{1}{a \cos \varphi} \frac{\partial}{\partial \theta} \left[p^* \frac{\partial z}{\partial \lambda} \right] - \frac{\partial}{\partial \theta}[mu\dot{\theta}].
\end{aligned} \tag{9.84}$$

The pressure-gradient term of (9.84) has a very simple and interesting form: It is proportional to the change with θ of the zonal mean of the product of the pressure and the slope of the height of the isentropic surface. The expression $\left[p^* \frac{\partial z^*}{\partial \lambda} \right]$ can be interpreted as “form drag” on the isentropic surface, analogous to the drag on mountains associated with the mountain torque, as discussed earlier in the course. Here the “mountains” are upward bulges of the isentropic surfaces, associated with blobs of cold air; the “valleys” are downward bulges of the isentropic surfaces, associated with blobs of warm air. We can say that

$$\text{upward flux of zonal momentum due to the wave} = - \left[p^* \frac{\partial z^*}{\partial \lambda} \right]. \quad (9.85)$$

Note that, from the perspective of isentropic coordinates, the upward flux of zonal momentum is associated with the pressure force, rather than with a covariance between the “vertical velocity” (which vanishes in isentropic coordinates in the absence of heating) and the zonal velocity. A layer of air confined between two isentropic surfaces will feel two momentum fluxes associated with the pressure force: one on its underside, and a second on its upper side. It is the difference between these two forces that tends to produce a net acceleration of the layer. That is why we see $\frac{\partial}{\partial \theta} \left[p^* \frac{\partial z^*}{\partial \lambda} \right]$ in (9.84).

Before completing our discussion of the Eliassen-Palm theorem in isentropic coordinates, it is useful to recall the form of the mechanical energy equation in isentropic coordinates, which was given in Chapter 2 and is repeated here for your convenience:

$$\begin{aligned} \left\{ \frac{\partial}{\partial t} (mK) \right\}_{\theta} + \nabla_{\theta} \bullet \{ m \mathbf{V} (K + \phi) \} + \frac{\partial}{\partial \theta} \{ m \dot{\theta} (K + \phi) \} + m \alpha \nabla \bullet (\mathbf{F} \bullet \mathbf{V}) \\ = - \frac{\partial}{\partial \theta} \left\{ -z \left(\frac{\partial p}{\partial t} \right)_{\theta} \right\} - m \omega \alpha - m \delta \quad . \end{aligned} \quad (9.86)$$

The first-term on the right-hand side of (9.86) represents the vertical transport of energy via “pressure-work.” The upward flux of wave energy is, therefore, given by $\left[-z \left(\frac{\partial p}{\partial t} \right)_{\theta}^* \right]$. Recall that for a neutral wave propagating zonally and vertically, with zonal phase velocity c , $\frac{\partial}{\partial t} = \left(\frac{[u] - c}{a \cos \varphi} \right) \frac{\partial}{\partial \lambda}$. It follows that

$$\text{upward wave energy flux} = \left(\frac{[u] - c}{a \cos \varphi} \right) \left[p^* \left(\frac{\partial z}{\partial \lambda} \right)_{\theta}^* \right]. \quad (9.87)$$

Comparing (9.86) with (9.87), we conclude that

$$\text{upward wave energy flux} = -\left(\frac{[u] - c}{a \cos \varphi}\right) \text{ times the upward wave momentum flux.} \quad (9.88)$$

This shows that for neutral waves propagating towards the east relative to the air ($-([u] - c) > 0$), the momentum flux and the energy flux have the same sign, while for neutral waves propagating towards the west relative to the air ($-([u] - c) < 0$) they have opposite signs.

Andrews et al. (1987) define a “mass-weighted zonal mean” of an arbitrary variable A by

$$[\hat{A}] \equiv \frac{[mA]}{[m]}. \quad (9.89)$$

Using the definition (9.89), we can write

$$mA = [mA] + (mA)^* = [m][\hat{A}] + (mA)^*, \quad (9.90)$$

$$\begin{aligned} [mAB] &= [mA][B] + [(mA)^* B^*] \\ &= [m][\hat{A}][B] + [(mA)^* B^*]. \end{aligned} \quad (9.91)$$

If we use (9.90) in (9.84), we get

$$\begin{aligned} \frac{\partial}{\partial t}([m][u] + [m^* u^*]) + \frac{1}{a \cos^2 \varphi} \left\{ \frac{\partial}{\partial \varphi}([mu\nu] \cos^2 \varphi) \right\} - [m\nu]f \\ = \frac{1}{a \cos \varphi} \frac{\partial}{\partial \theta} \left[p^* \frac{\partial z^*}{\partial \lambda} \right] - \frac{\partial}{\partial \theta} [mu\dot{\theta}]. \end{aligned} \quad (9.92)$$

Recall that the continuity equation in isentropic coordinates is given by

$$\frac{\partial m}{\partial t} + \frac{1}{a \cos \varphi} \left[\frac{\partial}{\partial \lambda}(mu) + \frac{\partial}{\partial \varphi}(m\nu \cos \varphi) \right] = -\frac{\partial}{\partial \theta}(m\dot{\theta}). \quad (9.93)$$

Taking the zonal mean of (9.93), we get

$$\frac{\partial}{\partial t}[m] + \frac{1}{a \cos \varphi} \frac{\partial}{\partial \varphi}([m\nu] \cos \varphi) = -\frac{\partial}{\partial \theta}[m\dot{\theta}]. \quad (9.94)$$

Subtract $[u]$ times (9.94) from (9.92), to obtain an “advective form:”

$$\begin{aligned}
& [m] \frac{\partial[u]}{\partial t} + \frac{\partial}{\partial t} [m^* u^*] + \frac{1}{a \cos^2 \varphi} \left\{ \frac{\partial}{\partial \varphi} ([muv] \cos^2 \varphi) \right\} - [mv]f \\
& - \frac{[u]}{a \cos \varphi} \frac{\partial}{\partial \varphi} ([mv] \cos \varphi) = \frac{1}{a \cos \varphi} \frac{\partial}{\partial \theta} \left[p^* \frac{\partial z}{\partial \lambda} \right] + [u] \frac{\partial}{\partial \theta} [m\dot{\theta}] - \frac{\partial}{\partial \theta} [mu\dot{\theta}].
\end{aligned} \tag{9.95}$$

Using the operations introduced in (9.90) and (9.91), we obtain

$$\begin{aligned}
& [m] \frac{\partial[u]}{\partial t} + \frac{\partial}{\partial t} [m^* u^*] + \frac{1}{a \cos^2 \varphi} \frac{\partial}{\partial \varphi} \{ ([m][\hat{v}][u] + [(mv)^* u^*] \cos^2 \varphi) \} - [m][\hat{v}]f \\
& - \frac{[u]}{a \cos \varphi} \frac{\partial}{\partial \varphi} ([m][\hat{v}] \cos \varphi) \\
& = \frac{1}{a \cos \varphi} \frac{\partial}{\partial \theta} \left[p^* \frac{\partial z}{\partial \lambda} \right] + [u] \frac{\partial}{\partial \theta} ([m][\hat{\theta}]) - \frac{\partial}{\partial \theta} ([m][\hat{\theta}][u] + [(m\dot{\theta})^* u^*]).
\end{aligned} \tag{9.96}$$

Dividing by $[m]$ and simplifying, we are left with

$$\begin{aligned}
& \frac{\partial[u]}{\partial t} + \frac{[\hat{v}]}{a \cos \varphi} \frac{\partial}{\partial \varphi} ([u] \cos \varphi) - f[\hat{v}] + [\hat{\theta}] \frac{\partial[u]}{\partial \theta} \\
& = - \frac{1}{[m]} \frac{\partial}{\partial t} [m^* u^*] + \frac{1}{[m] a \cos \varphi} \frac{\partial}{\partial \theta} \left[p^* \frac{\partial z}{\partial \lambda} \right] \\
& - \frac{1}{[m] a \cos^2 \varphi} \frac{\partial}{\partial \varphi} \{ [(mv)^* u^*] \cos^2 \varphi \} - \frac{1}{[m]} \frac{\partial}{\partial \theta} [(m\dot{\theta})^* u^*].
\end{aligned} \tag{9.97}$$

Here all of the eddy terms have been collected on the right-hand side.

Now define the isentropic Eliassen-Palm flux as

$$\begin{aligned}
\mathbf{F} &= (0, F_\varphi, F_\theta), \\
F_\varphi &= -a \cos \varphi [(mv)^* u^*], \\
F_\theta &= \left[p^* \frac{\partial z}{\partial \lambda} \right] - a \cos \varphi [(m\dot{\theta})^* u^*],
\end{aligned} \tag{9.98}$$

and its isentropic divergence as

$$\nabla_\theta \cdot \mathbf{F} = \frac{1}{a \cos \varphi} \frac{\partial}{\partial \varphi} (F_\varphi \cos \varphi) + \frac{\partial F_\theta}{\partial \theta}. \tag{9.99}$$

With these definitions, (9.97) can be written as

$$\begin{aligned}
\frac{\partial[u]}{\partial t} + \frac{[\hat{v}]}{a \cos \varphi} \frac{\partial}{\partial \varphi} ([u] \cos \varphi) - f[\hat{v}] + [\hat{\theta}] \frac{\partial[u]}{\partial \theta} \\
= -\frac{1}{[m]} \frac{\partial}{\partial t} [m^* u^*] + \frac{\nabla_{\theta} \cdot \mathbf{F}}{[m] a \cos \varphi}.
\end{aligned} \tag{9.100}$$

Consider a steady state (or time average) with no heating. Then the continuity equation (9.94) reduces to

$$\frac{\partial}{\partial \varphi} ([mv] \cos \varphi) = 0. \tag{9.101}$$

Since $[mv] \cos \varphi = 0$ at both poles, we conclude that $[mv] \cos \varphi = 0$ for all φ , or

$$[mv] = 0 \text{ for all } \varphi, \tag{9.102}$$

or

$$[v] = 0 \text{ for all } \varphi. \tag{9.103}$$

It follows from (9.100) that for steady flow in the absence of heating

$$\nabla_{\theta} \cdot \mathbf{F} = \frac{-1}{\cos \varphi} \frac{\partial}{\partial \varphi} [(mv)^* u^*] \cos^2 \varphi + \frac{\partial}{\partial \theta} \left[p^* \frac{\partial z^*}{\partial \lambda} \right] = 0. \tag{9.104}$$

In other words, for steady flow in the absence of heating, the divergence of the meridional momentum flux is balanced by the vertical derivative of the form drag.

9.7 The quasi-biennial oscillation

The zonal winds of the tropical stratosphere undergo an amazing oscillation with a period of about 26 months, called the “Quasi-Biennial Oscillation” or QBO. The QBO was discovered by Richard Reed in about 1960 (see the early review by Reed, 1965). The early evidence was not sufficient to establish the existence of a true oscillation in a statistically significant fashion, but additional decades of data have made it clear that a quasi-periodic oscillation really exists, as shown in Fig. 9.15. The observations show that a “ring” of air in the tropical stratosphere, extending over all longitudes, reverses the direction of its zonal motion roughly every two years. The oscillation is like a giant zonally oriented Ferris Wheel that periodically reverses the direction of its rotation. The winds shift from about 20 m s^{-1} westerly to 20 m s^{-1} easterly, and back again, so the changes are quite large. They are observed to propagate down from the middle stratosphere to near the tropopause. Corresponding oscillations are seen in other stratospheric fields, and to a much lesser extent also in the troposphere.

A theory of the QBO was proposed by Lindzen and Holton (1968) and Holton and Lindzen (1972). According to this theory, the oscillation is due to the interactions of upward-propagating Kelvin and Yanai waves with the mean flow. More recently, it has been proposed

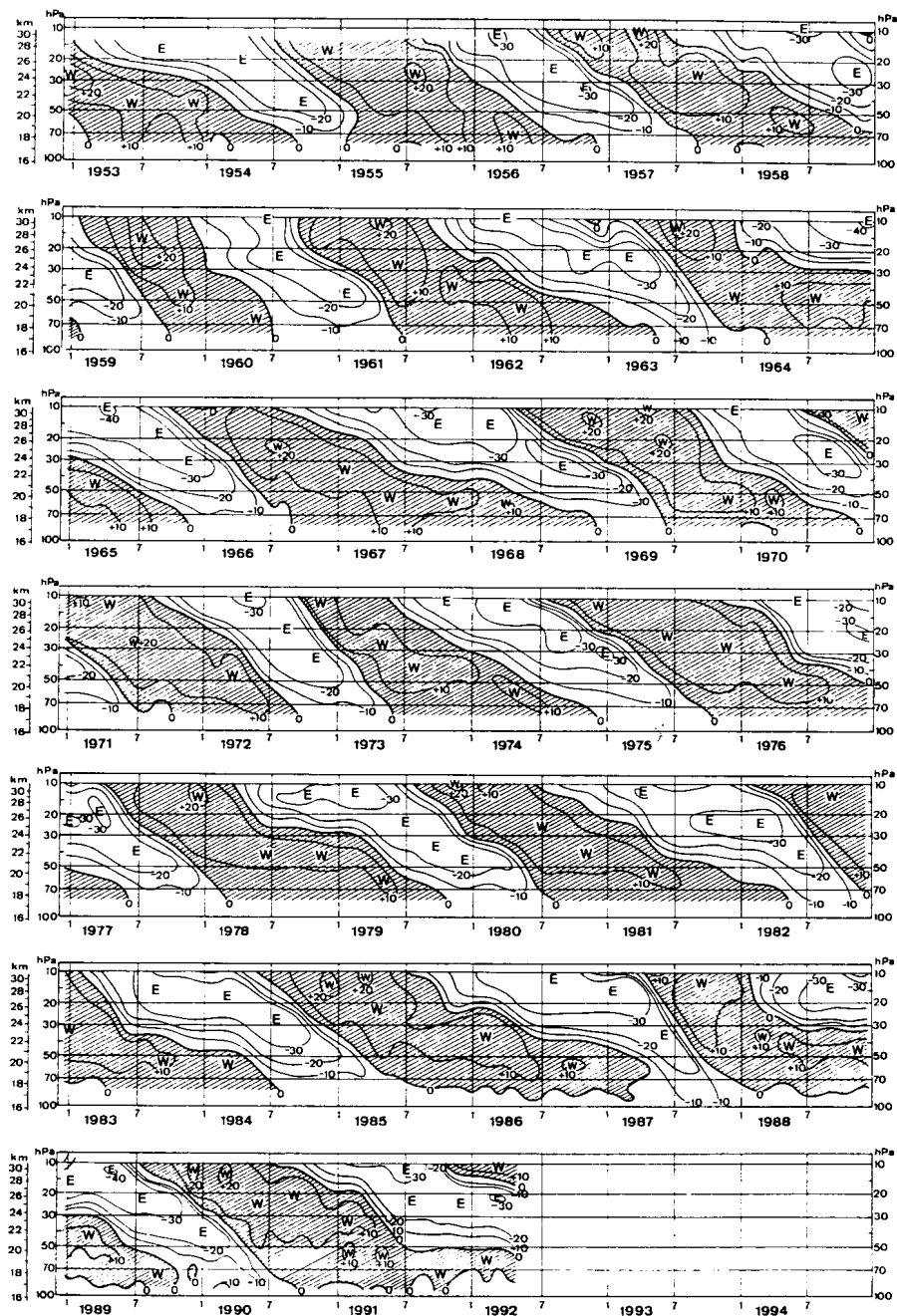


Figure 9.15: Time-height plot of the monthly mean zonal wind based on observations from various equatorial stations, namely Canton Island (January 1953 to August 1967), Maldive Islands (September 1967 to December 1975) and Singapore (January 1976 to May 1992). Contour interval 10 m s^{-1} , westerlies shaded. From James (1994).

that eastward- and westward-propagating gravity waves play an important role, and the Kelvin and Yanai waves are now being de-emphasized.

Both Kelvin waves and Yanai waves, which were discussed in Chapter 7, are observed to produce upward energy propagation into the stratosphere. The source of wave energy must, therefore, be in the troposphere, and is believed to be associated with cumulus convection. Each type of wave can be blocked by a critical level where $[u] - c = 0$; here c is the phase speed of the wave. Kelvin waves, with $c > 0$, can propagate through easterlies, for which $[u] - c < 0$, but not through westerlies strong enough to make $[u] - c > 0$. Because Kelvin waves propagate towards the east, relative to the mean flow, the “isentropic form drag” paradigm tells us immediately that upward propagating¹ Kelvin waves transport westerly momentum upward, i.e. they deplete the westerly momentum at lower levels, and deposit this momentum aloft, thus tending to produce westerlies aloft and easterlies below. They tend to produce a westerly acceleration at the base of a layer of westerlies. They therefore cause the westerlies to descend with time, as observed in the QBO. Recall that Kelvin waves do not involve fluctuations of the meridional wind; because of this they produce no meridional eddy transports of any variable. See Fig. 9.16.

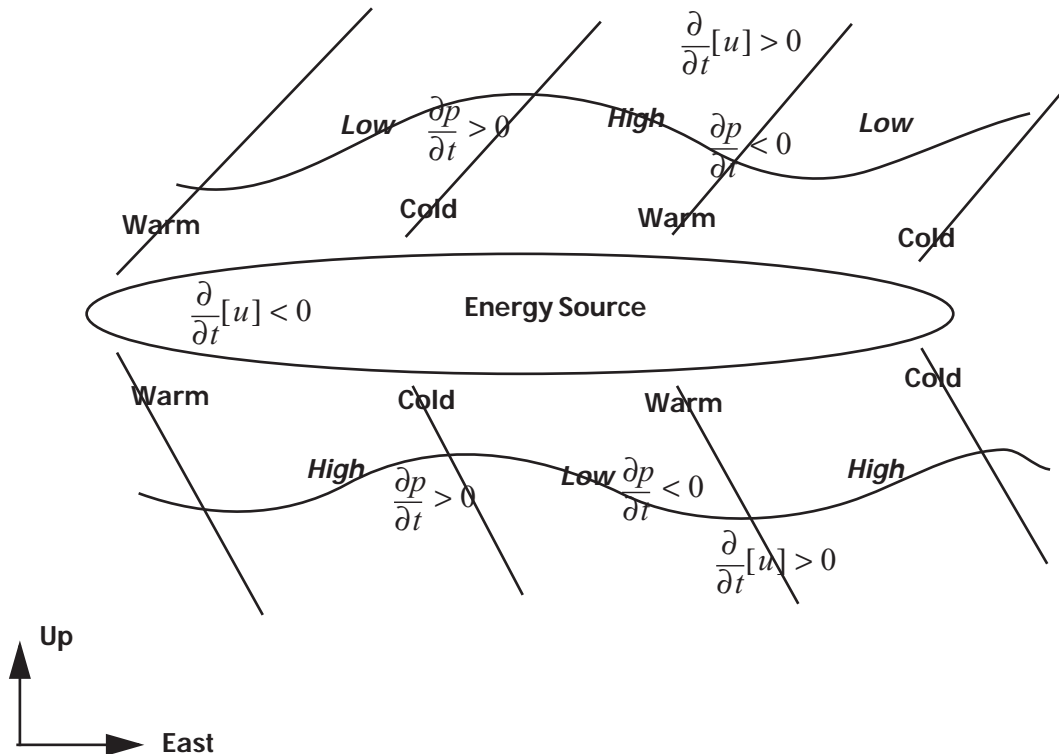


Figure 9.16: Energy and momentum fluxes associated with a Kelvin wave. The wavy lines show the heights of isentropic surfaces. Energy is propagating both upward and downward, away from the energy source. Where the energy flux is upward, the momentum flux is also upward, and vice versa. Westerly momentum is transported away from the energy source region, which feels an easterly acceleration to compensate.

¹. Here “upward propagating” means that the wave energy flux is upward.

Yanai waves, with $c < 0$, can propagate through westerlies, for which $[u] - c > 0$, but not through easterlies strong enough to make $[u] - c < 0$. Yanai waves that transport energy upward transport westerly momentum downward. The westward-propagating Yanai waves are damped in easterlies at the level where $[u] - c = 0$, and so they produce an easterly acceleration near the base of a layer of descending easterlies. Westward-propagating inertia-gravity waves will produce a similar effect, and recent work suggests that they are in fact important for the QBO.

Plumb (1984) produced a remarkable laboratory simulation of the QBO in an annular tank full of stratified salt water. In his experiment, “eastward” and “westward” propagating internal gravity waves are artificially excited by an oscillating diaphragm at the bottom of the tank. At a given level, the direction of the mean flow reverses periodically with time, and these reversals propagate downward. The oscillations are caused by wave-mean flow interactions.

For many years, atmospheric general circulation models failed to simulate the QBO. Recently, however, M. Takahashi (1996) has produced reasonably successful simulations of the QBO using a full atmospheric general circulation model of the troposphere and stratosphere. Earlier Carriolle et al. (1993) had produced a much weaker and less realistic but still promising simulation, and Takahashi and Shiobara (1995) had produced a QBO in a simplified GCM. During 1997, the ECMWF model began for the first time to produce a QBO when run in climate-simulation mode, i.e. without data assimilation. This improvement in the model’s performance was associated with an increase in the vertical resolution. It appears that high vertical resolution and possibly also weak damping are needed for a successful simulation of the QBO.

There is some evidence that a phenomenon similar to the QBO is at work in the atmosphere of Jupiter (Orton et al. 1994).

9.8 Blocking

Blocking (Rex, 1950 a, b) is a low-frequency, middle-latitude phenomenon characterized by a nearly stationary anticyclone that persists for at least several days and sometimes up to several weeks. The anticyclone splits the westerly jet and steers cyclonic disturbances around itself, mainly on the poleward side. The flow in the vicinity of a blocking high is strongly meridional, and is an example of what the older literature calls a “low index” regime. (A high index regime is strongly zonal.) Blocking highs tend to fluctuate in intensity, weakening briefly and then re-intensifying. They tend to remain nearly stationary in an average sense, although they may wander around a little over their lifetimes.

Blocks tend to occur preferentially in the Northern Hemisphere, and specifically in the eastern North Atlantic, the eastern North Pacific, and northern Asia. Southern Hemisphere blocking does occur, most commonly near New Zealand. Blocking can occur in both summer and winter, but is more common in winter. Wintertime blocking events sometimes appear to be associated with stratospheric sudden warmings (Quiroz, 1986). The formation of a block can be associated with upward propagation of a Rossby wave, which then interacts with the stratospheric zonal flow to produce a breakdown of the polar night vortex, i.e. a “Sudden Warming” event.

Blocks strongly influence weather patterns for one or more weeks at a time, sometimes in association with such things as persistent droughts (e.g. Green, 1977); if the formation and dissipation of blocks can be predicted, then weather patterns can be predicted with improved skill. Until recently, weather-prediction models were not very successful in forecasting blocks, and the same models run in climate simulation mode produced blocks less

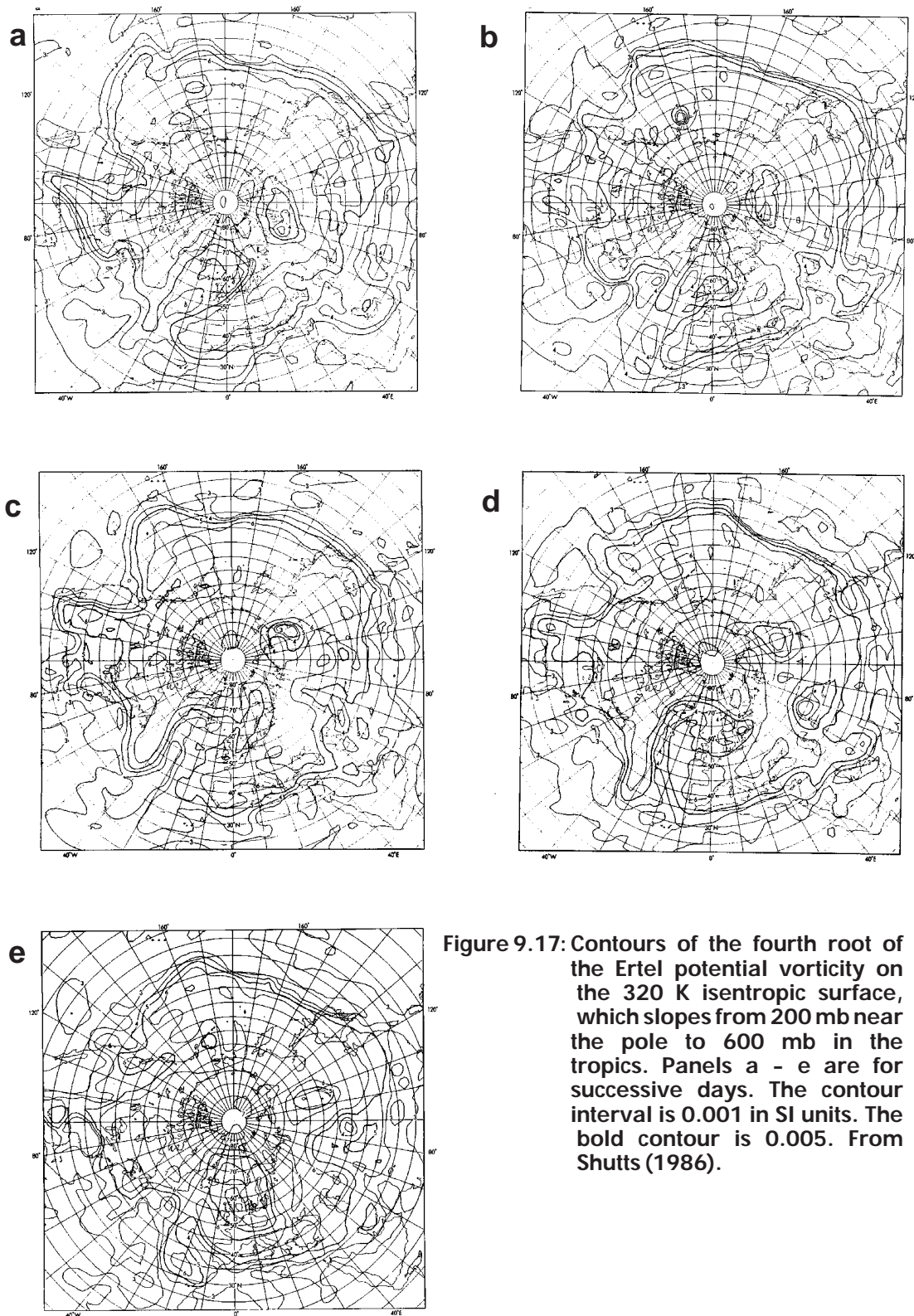


Figure 9.17: Contours of the fourth root of the Ertel potential vorticity on the 320 K isentropic surface, which slopes from 200 mb near the pole to 600 mb in the tropics. Panels a - e are for successive days. The contour interval is 0.001 in SI units. The bold contour is 0.005. From Shutts (1986).

often than observed. Within the last few years, this situation has improved dramatically, apparently as a result of increased model resolution.

What causes the formation of a blocking anticyclone? The current view is that blocks originate when particularly intense cyclones advect air with low Ertel potential vorticity from the subtropics (where low potential vorticity is the norm) into middle latitudes (where low potential vorticity is an anomaly). An example of this is shown in Fig. 9.17 taken from Shutts (1986). At the same time, a region of high potential vorticity air is advected into position on the equatorward side of the low potential vorticity anomaly. The block thus has a dipole structure in terms of potential vorticity. Near the longitude of the block, the potential vorticity decreases poleward, whereas it normally increases poleward. The blocking anticyclone could be called a “cut-off high,” while the cyclone is a “cut-off low.” Fig. 9.18 shows the

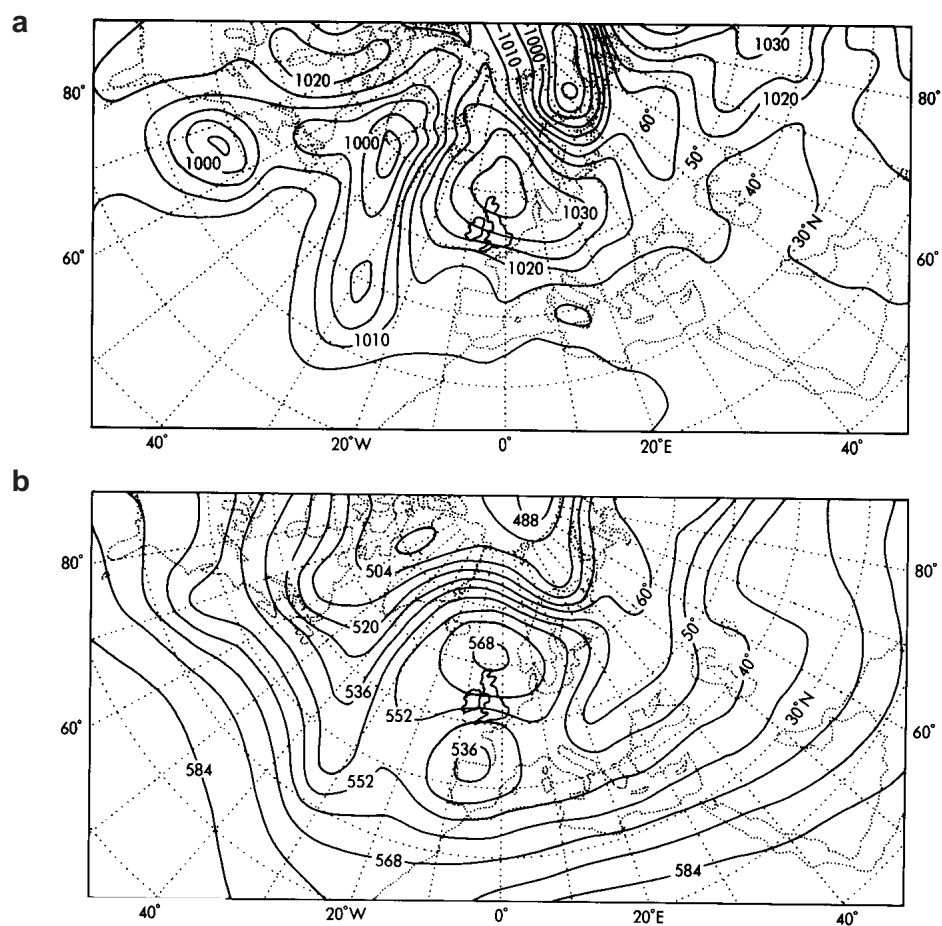


Figure 9.18: (a) Mean sea level pressure field for 15 February 1983, 12Z. Contour interval: 5 mb. (b) Height of the 500-mb surface for 15 February, 12Z. Contour interval: 8 dam. From Shutts (1986).

corresponding sea level pressure and 500 mb height fields. The dipole structure is clearly evident in the latter. Note that the westerlies have “split” into a strong branch to the north of the high, and a weaker branch to the south of the low.

In this example, a vigorous, short-lived, and small-scale cyclogenesis event (not shown in the figures) created a larger-scale anticyclonic perturbation that persisted for about 8 days, while the cut-off low survived for only about two days. How is it possible for blocking highs to persist as well defined, isolated “objects,” even while they are embedded in the turmoil of the midlatitude winter circulation? The destruction of the low seems natural; the persistence of the high demands an explanation. Hoskins et al. (1985) speculated that lows are disrupted by convection, while highs can survive because convection is suppressed there. Observations suggest that the smaller-scale transient eddies that are steered around a blocking high actually help to maintain the high. Blocks may therefore be examples of up-scale energy transport, which, as discussed in Chapter 9, is expected on theoretical grounds in two-dimensional turbulence. It has been suggested that blocking anticyclones in the Earth’s atmosphere are dynamical cousins of the “Great Red Spot” that has persisted in the atmosphere of Jupiter for at least several hundred Earth years.

There are two main theories of blocking dynamics, which look quite different but are not necessarily in conflict with each other. These are briefly summarized below.

Charney and DeVore (1979; hereafter CDV) suggested that in the presence of topography the large-scale circulation can adopt either of two equilibrium states, and that one of these corresponds to blocking, while the other represents a more typical and more zonal flow. The basic idea is that when the configuration of the mean flow is “right” there can be stationary waves that are resonantly forced by the topography. The waves feed back on the mean flow, however. Under certain conditions, the resonant waves alter the mean flow in a way that favors the formation of resonant waves, i.e. the waves create a mean flow that is favorable for their own continuing existence. On the other hand, if the waves are not present, the resulting mean flow is not favorable for the formation of the waves. Hence *the system can exist in either of two possible configurations*. These are referred to as “multiple equilibria.” Because the CDV theory involves the interactions of the waves with the mean flow, it is inherently nonlinear.

A simplified version of the CDV theory is as follows. The topography is assumed to vary sinusoidally in longitude, i.e.

$$h(x) \equiv h_T \cos(K_m x) . \quad (9.105)$$

The motion is described by a stream function, ψ , which is assumed to be of the form

$$\psi(x, y, t) = -U(t)y + A(t) \cos(K_m x) + B(t) \sin(K_m x) . \quad (9.106)$$

Think of this as a highly truncated functional expansion. The stream function is defined by the relations $u \equiv -\frac{\partial \psi}{\partial y}$ and $v \equiv \frac{\partial \psi}{\partial x}$; using these formulae, we see that the zonal component of the flow described by (9.106) is simply $U(t)$, i.e. it depends only on time. The “A” part of the wave is in phase with the topography, in the sense that for $A > 0$ the maximum of the stream function (corresponding to ridging behavior) occurs over the mountain. On the other hand, for $B > 0$ the “B” part of the wave represents a trough downstream of the mountain. The wave-like meridional component of the flow varies with both x and t :

$$v(x, t) = K_m \{ -A(t) \sin(K_m x) + B(t) \cos(K_m x) \} . \quad (9.107)$$

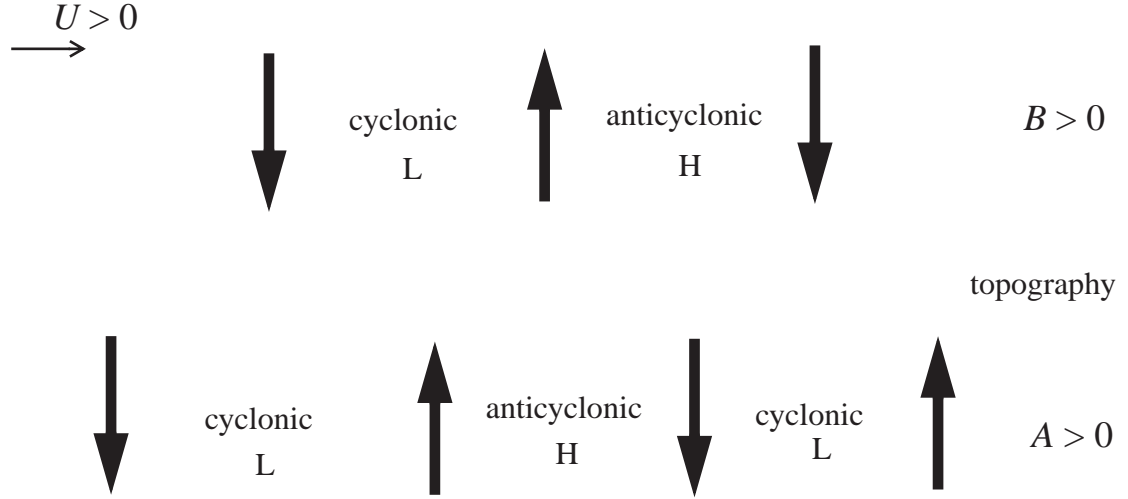


Figure 9.19: The relationships between the A and B components of the meridional wind and the topography in the model of Charney and Devore. The topography is indicated by the wavy line in the center. The arrows indicate the direction of the v -wind component, with “up” corresponding to “southerly.” The arrows above the topography are for the B -component of the wave, and the arrows below are for the A -component, assuming that A and B are positive. The indicated regions are cyclonic or anticyclonic for the case of $f > 0$ (the Northern Hemisphere).

By substituting (9.106) into a suitable nonlinear vorticity equation describing a Rossby wave flow with friction, CDV showed that the wave motion satisfies

$$\frac{1}{K_m} \frac{dA}{dt} + \left(\frac{\mathfrak{v}}{K_m} \right) A + \left(U - \frac{\beta}{K_m^2} \right) B = 0, \quad (9.108)$$

$$\frac{1}{K_m} \frac{dB}{dt} - \left(U - \frac{\beta}{K_m^2} \right) A + \left(\frac{\mathfrak{v}}{K_m} \right) B + \left(\frac{f_0 h_T}{K_m^2 H} \right) U = 0, \quad (9.109)$$

while the zonal flow obeys

$$\frac{dU}{dt} = \left(\frac{f_0 h_T K_m}{4H} \right) B - \mathfrak{v}(U - U^*). \quad (9.110)$$

In (9.109) - (9.110), the terms involving \mathfrak{v} represent friction. In (9.110), the “ B ” term represents the orographic form drag (or “mountain torque”) that the mountain exerts on the mean flow when the wave is oriented with the trough over the mountain, and the U^* term represents a “momentum forcing” that maintains the mean flow against friction. Note that (9.108) and (9.109) “blow up” if the wave number of the topography, K_m , is equal to zero.

This simply means that the wave solution does not occur in the absence of topography, i.e. the wave is topographically forced. Also note that (9.108) and (9.109) are nonlinear because they involve the products of A and B with U . This nonlinearity represents the wave-mean flow interactions.

CDV considered equilibrium (steady) solutions of (9.108)-(9.110). These equilibria can be found by setting the time-rate of change terms to zero, solving the resulting linear system (9.108)-(9.109) for A and B as functions of U , and selecting the appropriate value of U by requiring that (9.110) also be satisfied. Fig. 9.20 shows an example, in which the straight line represents the (B, U) pairs that satisfy (9.110), while the peaked line represents the (B, U) pairs that satisfy (9.108)-(9.109). There are three equilibria, but it can be shown that the middle one is unstable. The stable equilibrium with large U has a small wave amplitude, and the stable equilibrium with small U has a large wave amplitude. This is understandable because the wave term of (9.110) represents a drag on U . The solution with

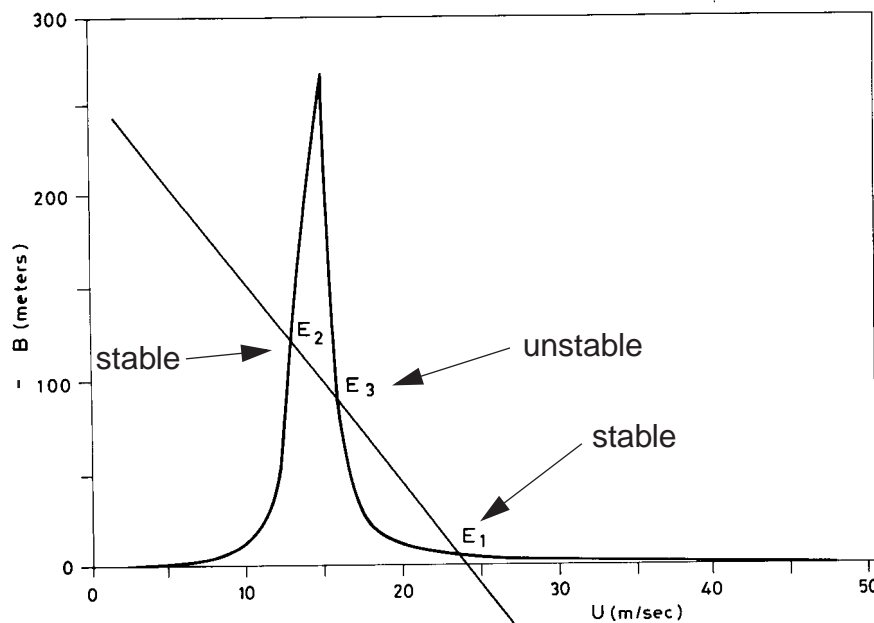


Figure 9.20: From Speranza (1986). Equilibrium solutions of (9.108)-(9.110), found by setting the time-rate of change terms to zero, solving the resulting linear system (9.108)-(9.109) for A and B as functions of U , and selecting the appropriate value of U by requiring that (9.110) also be satisfied. The straight line represents the (B, U) pairs that satisfy (9.110), while the peaked line represents the (B, U) pairs that satisfy (9.108)-(9.109). Evidently there are three equilibrium solutions, but it can be shown that the middle one is unstable.

large wave amplitude and a weak zonal flow is interpreted as representing blocking. CDV suggested that if the model is subjected to stochastic forcing, representing the random fluctuations of the weather, perhaps manifested through fluctuations of U^* , then the system can undergo occasional transitions back and forth between the neighborhood of the “blocked” equilibrium and the neighborhood of the “unblocked” equilibrium.

Charney and Straus (1980) extended the CDV theory to the baroclinic case, and it has been studied by many other authors. The CDV theory has been heavily criticized (e.g. Tung and Rosenthal, 1985), in part because its extreme idealizations limit the possible behaviors of the model, suggesting that the small number of discrete equilibria (i.e. two of them) is an artifact. Nevertheless the theory continues to be cited frequently as an important background concept for the interpretation of blocking. A number of authors have searched for evidence of multiple discrete equilibria in various datasets, with results that are suggestive but not entirely convincing.

McWilliams (1980) suggested that “modons” could be considered as idealized models of blocks. Modons are exact solutions of the nonlinear vorticity equation (Flierl, 1978). They have dipole structures, in which a high (a negative vorticity center) is paired with a neighboring low (a positive vorticity center). Modons must have finite amplitudes in order to exist; there is no such thing as a “linear” modon. An interesting property of modons is that they are resistant to disruption by perturbations. A modon “translates” relative to the mean flow. It is possible to set up a modon that is stationary relative to the Earth, in the presence of background westerlies. The conditions for this are special, however, and it is not clear why such special conditions should occur in real cases.

We can identify the following issues in connection with blocking, among others:

- What causes the formation of a blocking anticyclone?
- What determines the preferred geographical locations of blocking activity?
- How are blocking highs maintained against the noisy background flow?
- Why are blocks nearly stationary even though they are embedded in strong westerly currents?
- What causes the breakdown of a block?
- Why do we observe persistent, quasi-stationary anticyclones but not persistent, quasi-stationary cyclones?

The discussion given above shows that we have at least partial answers to some of these questions. We do not yet have a full understanding of blocking, however.

9.9 Summary

Waves and other eddies produce important effects on the large-scale circulation of the atmosphere. Important fluxes are associated with a wide variety of waves, including gravity waves, Rossby waves, and Kelvin waves. Momentum fluxes and temperature fluxes can tend to produce mutually counteracting effects, so that the mean zonal flow and temperature may not be altered. The appreciable effects of the eddies on the mean flow are typically associated with developing or decaying eddies, rather than steady, equilibrated eddies.

Two particularly important examples of wave mean-flow interactions in the general circulation are stratospheric sudden warmings and the quasi-biennial oscillation. Both involve wave propagation from the troposphere into the stratosphere.

Problems

1. Solve the one-dimensional Charney-Devore model, as given by the steady-state versions of Eqs. (9.108) - (9.110). Make a plot like that shown in Fig. 9.20. In order to do this you will have to choose appropriate values for the various parameters of the model. Explain your choices.

2. Show that $\psi_z^* = \frac{g}{f_0} \frac{T^*}{T_S}$.

3. Derive Eq. (9.17) of the notes.